Design of an Automated Ingestible Gastrointestinal Sampling Device

Yaw Amoako-Tuffour

Biomedical and Cell Therapy Research Laboratory

Department of Biomedical Engineering

Faculty of Medicine

McGill University

Montréal, Québec, Canada

A Thesis Submitted to McGill University in Partial Fulfilment of the Requirements of the Degree of

Master of Engineering

December, 2013

ABSTRACT

An ingestible, electromechanical capsule was designed to collect physical samples from the lumen of the human gastrointestinal tract with the aims of being able to better localize the source of gastrointestinal ailments, explore the microbiome, and monitor metabolic processes. A complete prototype was developed encompassing hardware, custom electronics, firmware and a novel sampling mechanism leveraging the cylindrical shape of the device. The prototype was assessed for its ability to collect samples and maintain their integrity; withstand the environmental conditions and forces associated with normal clinical use; and for its ability to transit safely through the gastrointestinal (GI) tract. The device was able to collect heterogeneous samples from an ex-vivo porcine intestine and maintain average sample cross-contamination of 7.58% over a 12 hour period at 37°C. The device was demonstrated to be an effective and non-invasive means to study the physiology of the GI tract and serve as a platform for further development in personalized medicine, drug delivery and GI intervention.

RÉSUMÉ ANALYTIQUE

Une capsule électromécanique ingérable a été conçue pour recueillir des échantillons physiques du tractus gastro-intestinal humain dans le but de mieux localiser la source des malaises gastro-intestinaux, d'explorer le microbiome et de surveiller les processus métaboliques. Un prototype complet a été développé incluant matériel, électronique sur mesure, logiciel et un mécanisme d'échantillonnage novateur tirant parti de la forme cylindrique de l'appareil. Des tests ont été effectués afin d'évaluer la capacité du prototype à prélever des échantillons et maintenir leur intégrité, supporter les conditions environnementales et les forces associées à l'utilisation clinique normale, et transiter en toute sécurité à travers le tractus gastro-intestinal. La contamination croisée a été plafonnée à 7.58% sur une période de 12 heures à 37 ° C. Et l'appareil était capable de prélever des échantillons hétérogènes. Il a été démontré que ce dispositif est un moyen efficace et non-invasif pour étudier la physiologie du tractus gastro-intestinal et servir de plate-forme pour le développement futur de la médecine personnalisée, l'administration de médicaments et d'intervention GI.

ACKNOWLEDGEMENTS

I would like to thank my supervisors Dr. Satya Prakash and Dr. Srikar Vengallatore for their support and guidance throughout the conceptualization and development of this project. I benefitted greatly from their expertise and experience. This work is supported by strategic research grant from Natural Sciences and Engineering Research Council of Canada (NSERC) to Dr. Prakash. Furthermore, I acknowledge and thank Micropharma for presenting me with the idea and the opportunity to work on this project. This project could not have been completed without the financial and human resources provided by Micropharma. Over the course of this project I have expanded my skillset to include mechanical design and fabrication, as well as become familiarized with microbiological concepts. With Micropharma I was able to identify the needs of industry and of the medical community, as well as gain exposure to the regulatory aspect of medical device development.

PREFACE

In accordance with the McGill University thesis preparation and submission guidelines, as stated in section I-C, I have take the option of writing this thesis as a compilation of original papers suitable for publications. The papers are presented in chapters 2, 3, and 4 and are subdivided into sections including abstract, introduction, materials and methods, results, discussion and conclusion. A common abstract, general introduction, literature review, summary of results, overall conclusions and references are included in the thesis as required by the guidelines.

LIST OF ABBREVIATIONS

BSH	Bile Salt Hydrolase
DBE	Double Balloon Enteroscopy
EM	Electromagnetic
HPLC	High-Performance Liquid Chromatography
HTS	High Throughput Study
IC	Integrated Circuit
ISFET	Ion Selective Field Effect Transistor
PCB	Printed Circuit Board
SPDT	Single Pole, Double Throw
USART	Universal Synchronous/Asynchronous Receiver Transmitter

Units:

V	volt
A	ampere
mA	milliampere
C	coulombs
mAh	milliampere-hour
cm	centimetre
mm	millimetre
N	newton
nm	nanometre

TABLE OF CONTENTS

LIST OF FIGURES AND TABLES

1. GENERAL INTRODUCTION

Diseases of the gastrointestinal tract contribute significantly to the global disease burden [1,2]. The gastrointestinal tract is also central to the maintenance of human health through mechanisms of its resident bacterial population and in its capacity as an interface for nutrient and waste exchange [3-5]. As the primary channel through which materials enter and exit the human body, the GI tract is a large repository of information and samples of the fecal matter, mucosa, luminal contents, and tissue provide insight to the health of the individual. In addition to serving as the site of nutrient absorption, waste expulsion, and as a major component of the immune defence system, the human gastrointestinal tract harbours a wealth of information pertaining to the health of individuals. Despite the major role of the GI in homeostasis, and the wealth of information held in its contents, available techniques for gastrointestinal exploration are unable to collect physical samples from the lumen of the entire gastrointestinal tract in a safe, convenient, and non-invasive manner. These techniques include: traditional and capsular endoscopy, colonoscopy, double-balloon enteroscopy (DBE), and stool sampling. Traditional endoscopy, in varying forms, has been in use since the early 20th century. It is based on a flexible tube with an internal lens system to allow visualization of the GI. Conventional endoscopes cannot explore the entire GI tract due to the difficulty in navigating the numerous and erratic bends of the GI system without significant risk of damage to the tract and patient discomfort [6-8]. Double Balloon Endoscopy (DBE) was developed during the 1990's and made commercially available by the year 2000 to extend the range of endoscopes[9]. Curves are navigated in DBE using 'push-and-pull' locomotion, however, the technique is time consuming (1.5 hours) and causes patient discomfort[9,10]. Capsular endoscopy is a relatively new method of visualizing the GI that miniaturizes the visualization capabilities of traditional endoscopes, however, it is currently unable to retrieve samples from the GI. Stool sampling is a common GI investigation method but is limited in the spatial and temporal information that it can provide from a given sample[11,12].

To overcome the limitations of existing gastrointestinal exploration devices, a new technology is required to provide improved access to the GI and its contents. An

autonomous ingestible device capable of collecting heterogeneous samples from the gastrointestinal tract during its transit would allow medical professionals and researchers to closely monitor reactions in the GI. It would provide localization and timing data on processes occurring in the gut and collect samples that would be isolated from downstream contamination and/or dilution. The combination of these features would facilitate targeted interventions in the GI, the discovery of new biomarkers, and the development of new therapeutics. This thesis documents the strategy, design, and development of such a medical device.

1.1 Research Objectives:

This project aims to address deficiencies in existing methods of studying, and intervening in the human gastrointestinal tract and the processes that occur therein. An ingestible medical device that is autonomous, and capable of collecting physical samples along the gastrointestinal tract addresses these issues well. The main objectives of the research are to:

(1) Identify the design requirements for this new class of ingestible medical devices; and
(2) Develop and test a prototype.

1.2 Thesis Organization

Chapter 2: Ingestible Gastrointestinal Sampling Devices: State of the Art and Future Direction (Literature Review)

This chapter reviews existing and proposed technologies for the purposes of exploring and intervening in the human gastrointestinal tract. It surveys general approaches and technologies used in the academic literature and patent space for developing ingestible medical devices. The purpose of this survey is to identify major challenges and promising avenues of development.

Chapter 3: Design Specification of an Ingestible Gastrointestinal Sampling Device

In this chapter, design requirements and features for the proposed medical device are explicitly developed. Minimum sample volumes needed to perform common bench-top analyses, typical gastrointestinal tract transit times, and biocompatibility standards determine the requirements. Constraints are set by physiological and anatomical constraints of the GI tract. The chapter steps through the development of each subcomponent (electrical, mechanical, and software) and describes their inter-relationships.

Chapter 4: Assessment and Optimization of Gastrointestinal Sampling Device Subsystems and Operational Performance

This chapter assesses the ability of the device's subsystems to perform to design specification. Through the construction and assembly of the device, design issues were identified and addressed in a process of system optimization. This process included software and hardware modifications, replacement of certain components, and adjustments to fabrication techniques.

CHAPTER 2:

Ingestible Gastrointestinal Sampling Devices: State of the Art and Future Direction (Literature Review)

Yaw Amoako-Tuffour, BEng [1], Mitchell L. Jones, MEng, MD, PhD[1,2], Nabil Shalabi, BEng, MEng [3], Alain Labbe, PhD[2†], Srikar Vengallatore, PhD[3], and Satya Prakash, PhD[1,2]*

Biomedical Technology and Cell Therapy Research Laboratory

Department of Biomedical Engineering and Physiology

Artificial Cells and Organs Research Centre

Faculty of Medicine

McGill University

3775 University Street

Montreal, Quebec, H3A 2B4

Canada

---

[1] Biomedical Technology and Cell Therapy Research Laboratory, Dept. of Biomedical Engineering, Faculty of Medicine, McGill University, 3775 University Street, Montreal, Quebec, H3A2B4, Canada. Tel: 1-514-398-3676, Fax: 1-514-398-7461, Email: satya.prakash@mcgill.ca; mitchell.jones@mcgill.ca

[2] Micropharma Limited, 141 avenue du President Kennedy, UQAM, Biological Sciences Building, 5th Floor, Suite 5569, Montreal, Quebec, H2X3Y7, Canada. Tel.: 1-514-987-4151, Fax: 1-514-987-4616, Email: mitchell@micropharma.net; satya@micropharma.net

[3] Department of Mechanical Engineering, McGill University, 817 Sherbrooke Street West, Montreal, Quebec, H3A2K6, Canada.

* Corresponding author;

2 LITERATURE REVIEW

2.1 Abstract

Despite the significant contribution of gastrointestinal diseases to the disease burden in North America, and the information contained in the gastrointestinal (GI) tract pertaining to other, delocalized diseases in the human body, conventional methods of exploring and collecting samples from the GI tract remain invasive and resource intensive. A new class of gastrointestinal sampling capsules is emerging in the literature containing the components required for an autonomous intra-luminal sampling capsule that preserves the spatial and temporal information of the gastrointestinal samples.

2.2 Introduction

Gastrointestinal diseases comprise a substantial portion of the global disease burden [1,2]. In North America and Europe, gastrointestinal cancers account for 25% of all cancer deaths [13]. Bacterial populations in the gastrointestinal tract also play an important though, as of yet, poorly understood role in gastrointestinal pathology and in the maintenance of normal physiological functions [3-5]. As the primary channel through which materials enter and exit the human body, the GI tract (or alimentary canal) is a large repository of information. Histological samples (i.e. tissue and mucosal) convey information on the disease state of the GI tract itself. Samples of its contents, investigated with analytic techniques such as qPCR, 16S pyrosequencing, and mass spectrometry among others may reveal biomarkers (marked increase or decrease in known analytes due to metabolic pathways perturbed by disease) from various locations throughout the body. These histological, morphological, and biochemical indicators of disease have historically been collected through fecal sampling, visualization, and various endoscopic-assisted biopsy techniques. Though effective, these techniques are invasive and often incapable of retrieving physical samples from the entirety of the small intestine (or maintaining spatial or temporal information in the case of fecal samples). Less invasive means of exploring the gastrointestinal tract would increase the frequency at which these investigations could be conducted and facilitate High Throughput Screening (HTS) required to study and identify new biomarkers.

In the year 2000, the first commercial endoscopic capsule was realized by Given Imaging (Yoqneam, Israel) [14,15]. This capsule made it possible to image the gastrointestinal tract (GI) non-invasively and throughout the GI tract including the entirety of the small intestine, a location never before fully attainable by the conventional tethered endoscopic devices [14,15]. Since then researchers have been developing technologies capable of performing a multitude of non-invasive procedures in the GI such as drug delivery, tissue biopsy, and with more versatile control over the locomotion and positioning of devices in the GI [15-20]. A function that has the potential to further the understanding of the GI is the collection of physical luminal content and lining. These materials contain elements of the microbiome, and metabolome that are potential biomarkers for disease. Biomarkers may indicate the future risk, or current progress, of a particular disease prior to the development of clinical symptoms and thus increase the likelihood of interventional success and a generally decreased morbidity associated with the disease. Collecting digestive fluid from the GI using stand-alone capsules has only briefly been mentioned in the literature [16,21]. To the best of our knowledge, only one stand-alone capsular device exists in the literature capable of performing fluid collection with in vivo sampling results [21]. However, numerous designs have been proposed for such a class of medical device in the literature and several of the disparate components required are actively being developed. This paper reviews the present state of the art in ingestible gastrointestinal sampling devices.

2.3 Gastrointestinal Sampling Device Design

Ingestible medical devices intended for clinical use must comply with guidelines set by the governing agencies in the target market (e.g. Food and Drug Administration). These guidelines specify the materials and technologies that may be used in the device, minimum safety standards, as well as limitations to its operation such as acceptable levels of interference that it may generate or receive. Chief among these guidelines is demonstration that the device causes no harm during the course of its operation and can perform, to a specified degree, its intended function(s). For minimally invasive gastrointestinal sampling devices, these guidelines translate into the following

requirements: Devices should be ingestible, capable of transiting safely though the GI, and retrievable; such devices should be designed to collect biologically relevant samples, whether liquid, solid, or a heterogeneous mixture, which may later undergo conventional and advanced analytical techniques; Sampling devices will be biocompatible and maintain structural integrity upon exposure to digestive and other bodily fluids; for clinical use, medical devices should have fault tolerance incorporated into the physical design and underlying software; Finally, the forces generated in the sample collection mechanism should be tolerable by the structures of the GI tract [22].

Dimensions

The pyloric sphincter, the most restrictive feature along the length of the human gastrointestinal tract, limits the dimensions of non-degrading ingestible devices [23]. However, the risk of capsule retention is present throughout the length of the GI, and may be elevated in patients with clinical histories of intestinal stenosis and Crohn's disease [24,25]. Commercial endoscopic capsules and "smart" pills designed for the adult population range in length from 18 – 35 mm and diameter from 6 – 12 mm [15,16,16,24,26-29]. The incidence of capsule retention for devices within these dimensions is reported as below 2% [30,31]. The lower limit for the dimensions of gastrointestinal sampling devices is the volume of biologically relevant sample required to perform the desired analysis. Sample volumes of 10-50μL are typical for qPCR [32].

Materials

Biocompatibility describes the absence of an adverse reaction, immunological or chemical, due to a given material in the presence of human bodily fluids [33,34]. These materials may range from degradable polymeric coatings, fluoropolymers, and elastomers, to durable thermoplastics, metal and glass [35-39]. Durable materials are preferred for the exterior of devices that are required to retain function and structural integrity throughout the length of the GI tract as is the case for endoscopic capsules,

monitoring pills, and gastrointestinal sampling devices. The use of different materials for various internal components may enable functionalization of specific surfaces for interaction with proteins, antibodies, and other biomarkers [40].

Control

The human gastrointestinal tract is broken up into anatomically and physiologically distinct segments that have vastly different tissues, anatomy, physiology and pathology. For some applications, the collection of eukaryotic cells leaving the sphincter of Oddi may be used to diagnose pancreatic disease, whereas collection just after the ileocecal valve may be used to diagnose colonic disease. These examples illustrate how the location and manner in which samples are collected impact the diagnostic power of gastrointestinal sampling devices. The control of sample collection is thus of central importance in the design of gastrointestinal sampling devices. Control is exerted through various means: Collection mechanisms aided by endoscopic imaging are under direct control of the physician. Upon visualizing the desired sample location, the physician can actuate the collection mechanism manually; Autonomous sample collection methods may employ mechanical systems, chemical compounds, and microcontroller units (MCUs) to control sample collection. A common control method for gastrointestinal sampling devices is the use of mechanisms triggered by the phase change of a chemical compound [41,42]. These chemical compounds are generally known as *enteric* compounds and undergo significant physical changes upon exposure to specific chemical compounds, enzymatic action, or environmental conditions [41]. The physical changes cause the release of the sampling mechanism. Enteric compounds are best suited for applications requiring low- to medium precision such as drug delivery in which compound degradation and absorption may span hours [42]. Electromechnical systems controlled by MCUs are advantageous in that they may be semi- or fully autonomous. These systems may be pre-programmed to react to specified environmental conditions, time, or location. They may also be triggered externally upon reaching the target location and have response times on the scale of microseconds[43]. For the improved precision and autonomy afforded by electromechanical designs, it is believed that the feasible course for ingestible

gastrointestinal sampling devices is embedded microcontroller units for system control. The design considerations for an electromechanical sampling mechanism include: power, localization, telemetry, signal processing, mechanical actuation and the ability to sense environmental conditions.

Locomotion

Gastrointestinal sampling collection techniques based on endoscopy or double balloon enteroscopy, (or any tube-based technique) reach their target location through the application of force at the proximal end of the device. The majority of ingestible electromechanical sampling devices reach their target locations, and continue to transit through the GI tract, passively under the force of peristalsis [28,44,45]. Passive locomotion requires no propulsive hardware but may be erratic. A number of active locomotion techniques have been developed for ingestible capsules including: 1) micro-mechanical legs, paddles, or propellers [44,46-48]; (2) the controlled expansion of compressed gas to provide propulsion [17]; or (3) utilizing propulsive forces transmitted by an external system, typically a magnetic field, in which devices have embedded magnets or coatings and are directed with an external magnetic driving device [49-51]. Furthermore, modifications to the material surface properties of a device could influence locomotion, such as micro-pillar polymer arrays coated with viscous oil that could improve adhesion to the microvilli of the intestinal mucosa [52-54].

Localization

Device localization and accurate timing are critical in determining the site and rate of metabolic reactions. This information may be utilized prior to ingestion to target locations for sampling, or it may be used following retrieval to trace the source of the samples. Measuring position in the GI in 3-Dimensional space, distance traveled along tract, or the location of certain regions in the GI has proven difficult as the GI is a long tubular structure that folds upon itself and is largely free to move within the abdominal cavity with few fixed points [55]. Nonetheless, methods have been developed to track devices inside the tract include timing, computer vision, triangulation methods, inertial

navigation and external monitoring [49,50,56-58]. Due to the long transit time of the medical device along the gastrointestinal tract, it is not feasible to have a human operator present throughout the course of operation. For this reason, autonomous localization methods are considered the viable option for these devices and this precludes the use of external imaging or tracking systems requiring human operators.

The most basic form of localization uses typical gastric and small bowel transit times as guidelines to determine the physical location of the pill at a given time point. This method is prone to error as an individual's transit time may vary significantly from the statistical norm and indicate erroneous locations. It may however, be possible to standardize transit times through dietary restriction (e.g. fasting state), bowel preparation and/or co-administration with prokinetic agents such sodium phosphate to help the motion of the device by overcoming stoppages at sphincter regions[15,59].

Inertial navigation and positioning systems are based on the integration of measurements from an array of on-board multi-axial accelerometers and gyroscopes [60,61]. This method, however, is computationally intensive and susceptible to compounding error over extended periods due to the number of measurements and irregular movement inside the GI [62].

Computer vision is being developed as a means to retroactively determine the location of endoscopic capsules. During the course of transit, an endoscopic capsule may take between 40,000 – 60,000 images which are later reviewed for abnormalities[63]. To reduce the time required to review these images, algorithms based on pattern recognition and texture analysis have been demonstrated to accurately segment the GI tract into distinct anatomical regions of interest [63-65]. Despite the success of these techniques in the post-procedural review, they rely on external computation and are unable to provide real-time/actionable data to the transiting medical device and thus cannot be utilized for targeted sample collection.

A number of triangulation methods, analogous to the Global Positioning System (GPS), have been used to localize ingested capsules in 3D space [57,58,66]. Received Signal Strength Indication (RSSI) uses the ingested device as an RF emitter and an external

sensor array to measure RF signal strength at fixed locations on the abdomen. The relative signal strengths are used to calculate the 3D position of the device[66]. The average error with this method reaches 37.7 mm due to varying signal attenuation by the differing body tissues [16]. Time of Arrival (TOA) is another form of triangulation in which the three-dimensional position of the sampling device is calculated from the difference in reception time of an EM signal at three receivers located externally on the abdomen. A high degree of synchronization (within 1 ns) of the receivers is required to achieve 0.3 m resolution [67]. Magnetic tracking is also immune to attenuation by body tissue and uses the field strength generated by a permanent magnet inside the device and detected by a skin-mounted magneto-resistive sensor array to estimate 3D position with 3.3 mm error [16,57]. It has the advantage of not increasing power consumption of the device, but it is susceptible to interference by external magnetic fields and high-voltage electrical devices. Furthermore, the large permanent magnet diminishes potential sampling volume within the device. A general weakness of triangulation methods is the positional error that occurs due to natural body movement. Changes in the relative positions of the external reference points will vary with torso movement and thus produce erroneous device locations[68].

Conventional clinical imaging may be used to localize sampling devices when seeking to maximize available sample volume in the capsule. Ultrasound imaging is based on ultrasonic pulses emitted from outside the body and echoed by the device using low frequencies (100 kHz to 5 MHz) [17] and has been demonstrated as an effective localization method for medical devices within the GI [69]. Radioactive tracers may also be placed in compartments within the medical device such that its transit through the GI may be tracked by gamma cameras [70]. However, imaging methods based on ionizing radiation, including X-ray, are not suitable for continuous device tracking.

Sense Environmental Conditions

Environmental sensors provide a means of device localization within the GI tract and facilitate real-time decision-making based on the surrounding environment. Parameters typically measured include: gastrointestinal pH [71], pressure [72], temperature [73,74], oxygenation and oxidation/reduction using cyclic voltammetry, and electrical

conductivity [14,75]. The concentration of hydrogen ions (pH), can be measured using antimony and glass pH electrodes, and Ion-Sensitive Field-Effect Transistors (ISFET) which have been implemented in a number of ingestible devices, including the SmartPill® GI Monitoring System (Given Imaging, Israel) and the Phillips-Medimetrics device [75-78]. PH sensing can be used as part of a diagnostic paradigm and, when combined with time, can be used to provide localization information for the delivery of a drug or the acquisition of a sample as described above [79]. It should be noted, however, that ISFET pH sensors are sensitive to changes in temperature and must be calibrated at regular intervals to provide accurate pH measurements [80].

Temperature measurement is performed using thermistors, Resistive Thermal Devices (RTDs), as is the case in the VitalSense® ingestible telemetric physiological monitoring system pill (Mini Mitter Co., Inc., Bend, OR) [81], or by monitoring frequency shifts in temperature sensitive crystals such as is employed by the CorTemp® Pill system by HQ Inc (Palmetto, FL, USA) [20]. Silicon diode temperature sensors, and forward biased pn junctions have also been used to serve this purpose [75,78].

Radiant energy has also been proposed as a means of environmental sensing for ingested devices. These technologies include: fluorescence endoscopy, optical coherence tomography, confocal micro-endoscopy, light-scattering spectroscopy, Raman spectroscopy, and molecular imaging for optical biopsy or the use of transmission spectroscopy for detecting intestinal bleeding [82,83].

Telemetry

Endoscopic and monitoring capsules routinely employ wireless communication to transmit and receive commands and to offload data logs and images [84,85]. A major design consideration is the extent to which data transmission rate and transmission distance affect power consumption. Wireless signals from ingestible medical devices must not interfere with standard hospital equipment but must be sufficiently robust to overcome external interferences. The dedicated RF communication standard is the Medical Implant Communication Service, operating in the 402–405 MHz range, although other Industrial

Scientific and Medical bands such as 433.92 MHz are acceptable [86,87]. Several systems use electric-field propagation that exploits the human body as a conductive medium for data transmission which may offer higher data rates with lower power consumption than existing RF technologies due to the elimination of power consuming RF transmission components [20].

Power Supply

The power supply for electromechanical gastrointestinal sampling devices may be integrated into the device, or disconnected and external to the device. Silver oxide coin-cells and lithium polymer batteries are commonly used internal power supplies in ingestible and implantable medical devices [43,88,89]. To achieve compact designs, to power inaccessible devices such as permanent implants, and/or to power devices with high-energy consumption, external power supplies may be utilized. Wireless energy transmission through biological tissue is achieved by creating an inductive link between an external primary coil (worn around the patient's torso) and a secondary coil (embedded within the capsule) [28,90,91]. Excitation of the primary coil will induce electrical current in the secondary coil providing power to the device. Although external power supplies offer internal space savings and extended operation capabilities by virtue of a larger power supply, the raise design complexity and diminishes the ease of use due to additional supporting infrastructure.

Sample Collection

Sample collection can be described as either having an active or passive mechanism. Active mechanisms generally feature a high level of control and the potential to gather heterogeneous sample material. Passive mechanisms, however, do not require power supplies and may be made more compact and simple in their design. For the purposes of this review active sampling mechanisms are identified as those requiring the controlled

release of mechanical energy to collect sample from the lumen of the gastrointestinal tract.

Several active sampling mechanisms for ingestible capsular devices have been described in the literature utilizing: shape memory alloys, compressed springs, air pressure, motors, and elastic materials to actuate plungers, pistons, and biopsy forceps [92-95]. Electric thermoactuators are often used to trigger the release of stored mechanical energy by destroying a degradable material (e.g. nylon monofilament) that holds the actuating element in a "high-energy" state [21]. Shape memory alloys are unique in that they undergo conformational changes with the application of electrical current and do not require a secondary trigger to release mechanical energy. A number of micropumps have been proposed for fluid sampling and drug dosing in smart pills. These include mechanical pumps based on electrostatic and piezoelectric forces and non-mechanical pumps based on electrokinetic principles such as electroosmosis [96]. Though the mechanical micropumps have been demostrated to achieve high pressures (31 kPa) and flow rates (850μL/min) they require very high supply voltages (200 V) to operate [97]. Non-mechanical micropumps or electrokinetic pumps such as those driven by electroosmotic, capillary, or electrohydrodynamic forces require fluid that is polar, free of particulate matter, and non-viscous [96]. These requirements preclude the heterogeneous and highly variable luminal contents of the gastrointestinal tract.

Passive collection mechanisms include microfluidic capillary tubes and the selective exposure of absorptive materials to the fluid of the GI [98,99].

2.4 Current GI Sampling Capsules

In 1996, Howard et. al applied for a patent describing a pill shaped container with a hollow body, opening, seal, and a vacuum interior [98]. Upon reaching the target sampling location, indicated by pH, enzymatic activity, or the presence of a particular chemical compound, the seal would dissolve allowing intraluminal contents to enter the storage area. The capsule could be subdivided into as many as 3 sub-compartments each with their own vacuum, opening, and seal. The seals are of different thicknesses meaning that

they would degrade at different times and thus allow the administrator to collect samples from different locations along the GI tract. Enteric compounds are also used as seals in microfluidic sampling devices. In a patent application by Sprenkels et. al, a microfluidic-based GI fluid sampling concept is described that uses capillary forces to draw in samples from the GI [99]. Prior to administration, the channels would be sealed with enteric compounds sensitive only to the fluids targeted for sampling collection. Upon contact with these fluids, the seals would dissolve and allow the passage of fluid into the channels under capillary motion. These devices offer passive, solid-state designs that are independent of external infrastructure. However, there are a number of issues with these devices that make them poorly suited for the purposes described in this paper. In both design categories, there is no provision made for re-sealing the chambers following sample collection and thus leading to downstream contamination. Furthermore, the designs require *a priori* knowledge of the target fluids and cannot accommodate variations in viscosity, physical, and chemical composition of the fluid in the GI tract.

In a sampling capsule designed by Cui et. al, a MEMs calorific element causes the release of a piston. As the piston advances, the device simultaneously elutes medication into the GI and draws luminal content into the sampling chambers[21]. As the drug exits the primary aperture, the volume is displaced by liquid drawn in through apertures along the sides of the capsule. At 10.2 mm in diameter and 30 mm in length, the polycarbonate capsule elutes an average drug volume of 0.498 mL and captures an average sample volume of 0.262 mL. The device uses a micro-scale magnet marker inside the device and a location monitoring Hall sensor array fixed on a waistcoat worn by the subject to track its position in the GI tract. Commands are transmitted to the device from an external RF signal emitter and it is powered internally by three 1.55 V, 40mAh silver oxide batteries (9.5-mm × 2.09-mm). This design features many important elements for autonomous gastrointestinal sampling such as GI localization, wireless communication, and large sample volume. However, the device is limited to collecting a single liquid sample that is not isolated from down-stream contaminants. The liquid-only sampling is a source of bias as information in the mucosa and solid materials in the GI will remain inaccessible.

Additionally, its small ports are susceptible to obstruction by particulate matter. These limitations reduce the device's utility as a research and diagnostic tool. A similar phase bias exists for another mechanical sampling tool, designed by Park et al in 2008, which uses a torsion spring to perform tissue biopsies in the GI [94]. This sampling tool was designed as an "add-on" to augment the capabilities of existing endoscopic capsules. The sampling mechanism consists of a torsion spring held under tension by a polymer string. The torsion spring is released when current is passed through a resistive heater to break the polymer string. The torsion spring drives a slider-crank mechanism that converts rotary motion into linear motion. The oscillating linear motion drives a toothed lance that extends into the lumen of the GI tract and retracts into the body of the capsule with tissue trapped in its teeth.

A concept for an advanced sampling capsule was described in a 2003 patent application by Tang et. al. which utilizes counter-rotating cylindrical blades to collect samples from the lumen of the gastrointestinal tract [95]. It is designed as an in-vivo diagnostic tool with an on-board micro-spectrometer, biosensors, and a specimen collection device capable of transmitting information wirelessly to an external receiver. Though this design is yet to be realized and its efficacy remains unproven it is notable for its use of miniature motors in its collection mechanism.

2.5 Future Direction

With the high disease burden associated with gastrointestinal ailments and the potential to infer other disease states from biomarkers and microbiome found in the gastrointestinal tract, the need for non-invasive GI sampling techniques is definitive. Existing gastrointestinal exploration techniques such as endoscopy, colonoscopy, and double-balloon enteroscopy are capable of collecting luminal and tissue samples for biopsy from much of the digestive tract but they are invasive, resource-intensive, and thus ill-suited for high throughput research required to identify novel biomarkers and observe physiological processes in the gastrointestinal tract. These limitations also make the existing methods unsuitable as easily administered diagnostic, monitoring, and

intervention tools. The future of gastrointestinal exploration lies in small, autonomous sampling devices that may be targeted and lend greater specificity and sensitivity to researchers over existing methods. A review of the literature revealed numerous approaches to this challenge. Based on this review, and in light of the design considerations outlined earlier in this document, it is the author's conclusion that a feasible solution for an autonomous gastrointestinal sampling device will be: 1) an electromechanical device controlled by an onboard microprocessor, 2) equipped with an internal power supply, 3) positioned within the gastrointestinal tract using a combination of time and localized environmental changes, 4) subject to passive locomotion along the gastrointestinal tract, and finally 5) equipped with an active sampling mechanism to accommodate a diversity of sample materials. For heightened efficacy, the device will collect multiple, and discrete, samples that will be isolated from contaminants until their due recovery. Beyond the development of a candidate device, the collected samples must be characterized to ensure that they are representative of the locations that they are meant to be sampling. The continued development of this device class will lead to a greater understanding of the relationship between the gastrointestinal contents and various disease states and serve as a powerful research tool in the discovery of biomarkers and development of novel therapies.

2.6 Acknowledgements

The author acknowledges contributions from Nabil Shalabi from the lab of Dr. Srikar Vengallatore in the Department of Mechanical Engineering at McGill University.

2.7 Research Justification:

There have been numerous developments in the domain of gastrointestinal sampling. However, there currently exist no devices that meet all of the required specifications for a viable gastrointestinal sampling capsule. The reviewed devices are incapable of collecting multiple heterogeneous samples of sufficient volume in a non-invasive manner, and they are incapable of preventing contamination or dilution of the samples

once they have been collected. Further integration of the disparate technologies, and the creation of new technologies are required to achieve the stated goals of this thesis.

CHAPTER 3:

Design of an Ingestible, Electromechanical Capsule for Gastrointestinal Sample Collection (for GI Luminal Fluid Sampling)

Yaw Amoako-Tuffour, BEng [1], Mitchell L. Jones, MEng, MD, PhD[1,2], Alain Labbe, PhD[2†], and Satya Prakash, PhD[1,2]*

Biomedical Technology and Cell Therapy Research Laboratory

Department of Biomedical Engineering and Physiology

Artificial Cells and Organs Research Centre

Faculty of Medicine

McGill University

3775 University Street

Montreal, Quebec, H3A 2B4

Canada

---

[1] Biomedical Technology and Cell Therapy Research Laboratory, Dept. of Biomedical Engineering, Faculty of Medicine, McGill University, 3775 University Street, Montreal, Quebec, H3A2B4, Canada. Tel: 1-514-398-3676, Fax: 1-514-398-7461, Email: satya.prakash@mcgill.ca; mitchell.jones@mcgill.ca

[2] Micropharma Limited, 141 avenue du President Kennedy, UQAM, Biological Sciences Building, 5th Floor, Suite 5569, Montreal, Quebec, H2X3Y7, Canada. Tel.: 1-514-987-4151, Fax: 1-514-987-4616, Email: mitchell@micropharma.net; christopher@micropharma.net; satya@micropharma.net

* Corresponding author;

Key terms: medical device, ingestible capsule, gastrointestinal, sampling.

3 CHAPTER 3: Design of an Ingestible Gastrointestinal Sampling Device

3.1 Abstract

The human gastrointestinal tract is a repository of health information. Imbalances in bacterial populations or the presence of biochemical markers can indicate disease and should be sought out for early detection. Existing methods of gastrointestinal exploration are incapable or retrieving physical samples from the small intestine in a convenient and information-preserving manner. To address these limitations, an electro-mechanical ingestible capsule was designed to acquire samples from targeted locations along the gastrointestinal tract. Following several design iterations, a solution based on a rotary collection mechanism was developed. Two, separate, embodiments of the candidate device each contain an actuation mechanism, sample storage, on-board power supply within ⌀11mm x 31 mm and ⌀13.65mm x 34.96mm capsules. The candidate device is programmable via infrared light and contains three sampling chambers, each with 83.8 μL capacity capable of collecting and maintaining discrete samples.

3.2 Introduction

3.2.1 Gastrointestinal Anatomy and Physiology

The human gastrointestinal is comprised of the mouth, oesophagus, stomach, small intestine (duodenum, jejunum, ileum), large intestine (caecum, colon, rectum) and the anus. Areas of particular interest are the small intestine and colon where the majority of nutrients are absorbed and where beneficial bacteria reside respectively[100,101]. The length of the small intestine ranges from 3m (*in-vivo*) to 7m and has a diameter of 5cm[102]. A cross-section reveals layers of smooth and circular muscle surrounding a tubular tissue structure normally in a collapsed state. The internal portion of this tubular structure is referred to as the lumen and is lined with a thick layer of mucin – a water-insoluble free flowing and viscous gel, which protects the underlying epithelial surface from damage due to abrasion or harsh chemicals[103]. Transit times vary within and across individuals due to factors such as diet and exercise. Different sections of the GI also possess unique flow rates. For instance, the jejunum has a flow rate of 2.52 ml/min and the ileum 1.23 mL/min. The gastric phase of digestion is largely determined by the structure and

consistency of the stomach's contents which are held until degraded into sufficiently small particles that may be passed to the small intestine. Liquids pass faster than solids which typically take from 2-5 hours to transit. Following passage through the pyloric sphincter, the bolus travels through the small intestine and has the majority of its nutrients absorbed before finally reaching the cecum after 3-6 hours[104]. The large intestine has the greatest variation in residency time ranging from a few hours to days. Total transit time in humans is approximately 20-30 hours; however, it is possible to have material reside in the colon from 8 hours to 72 hours[104]. Food products are moved along the gastrointestinal tract in a process known as *peristalsis*. Peristalsis is the coordinated movement of circular and longitudinal muscles acting along the GI to transport food products.

An estimated 10^{13} - 10^{14} bacteria reside in the GI tract and are collectively known as the *microbiome/microflora*. They represent between 400-500 species and are found primarily in the colon and to a lesser extent in other regions of the GI[105]. The distal small intestine (ileum) acts as a transition zone from the upper small intestine where only acid-tolerant lactobacilli and streptococci reside. Microflora play an important role in maintaining human health, however the mechanisms through which it influences health are poorly understood [102,106,107]. They may be categorized as either *Autochthonous* or *Allochthonous*. *Allochthonous* bacteria are transient *whereas Autochthonous* bacteria are permanent and perform functions such as the synthesis of vitamin B12 and vitamin K[108-110]. They also bestow a level of immunity upon the host by preventing the colonization of the GI tract by pathogenic microbes[4]. Perturbations to the microflora may be caused by the administration of broad-spectrum antibiotics, chemical therapeutics, radiation, as well as diet modification and the introduction of new and viable bacterial populations[111-114].

3.2.2 Critical Subsystems and Components

A candidate device designed to autonomously sample the contents of the human gastrointestinal tract will be internally comprised of four major sub-systems: 1) System control, 2) sampling mechanism, 3) localization method, and 4) a power supply. Two or more of these subsystems may overlap. For instance; enteric triggers may serve as both system control and as a localization method[115]. Additionally, the power supply need not

be electrical or chemical. Stored mechanical energy such as compressed springs may also be appropriate.

3.2.3 Design Specifications

Dimensions

Dimensional constraints were among the first design considerations. They were limited by human anatomy and influenced which internal components may be included in the design. Precedent had been established by the manufacturers of endoscopic capsules whose devices have gained regulatory approval[116]. For this reason, the upper bounds of 13 mm x 30 mm (diameter x length) were selected as the target for the candidate device.

Physician Workflow Constraints

The next consideration is the manner in which the device is to be used by health professionals and researchers. In a research environment, it may be feasible to oversee the administration and transit of a device. However, in clinical settings physicians are unable to monitor the patient as the capsule transits to the appropriate location along the GI. The success of devices such as the Smart Pill is partly due to the quick turn-around time with the patients. Consultation with gastroenterologists confirmed that the structure of a typical workday does not accommodate seeing patients multiple times a day and at irregular hours. This reality ruled out designs dependent upon external imaging such as x-ray, MRI, or ultrasound for localization. External triggering mechanisms were also ruled out meaning that the device would have to be developed in a way that would allow self-triggering at the appropriate location(s).

Sampling Requirements

A minimum of three samples collected by each capsule during transit will allow the investigator to span an anatomical range or to target a specific location in triplicate. Each sample should remain discrete and independent of the others to ensure that they are representative of the source. A primary goal of the device is to locate, quantify, and characterize the human microbiome. Quantitative PCR (qPCR) and 16S pyrosequencing are well suited to analyse the recovered samples using volumes of ~ 30-100 µl [117].

Longevity

The candidate device should be able to collect samples at any point along the GI. With average transit and residency times of 20-30 hours, the target battery life was set to 30 hours[104]. Excess capacity will be used to maintain a beacon for easy identification and retrieval as well as to off-load logged data. Longevity implicitly describes the ability of the device to withstand the environmental conditions and maintain it's structural integrity as it transits. Inert, biocompatible materials must be used for sections that come into contact with the GI environment and reasonable steps must be taken to ensure that the internals remain free of external fluids.

Customizability

Customized run-time parameters such as location, time, environmental conditions, and sampling duration may be achieved through unidirectional or bidirectional wireless communications protocols.

3.3 Hardware Design

3.3.1 Sample Collection Mechanism

The sample collection mechanism, being central to the device, was the first subsystem to be developed. Several mechanisms were explored with the criteria that the mechanism be compact, capable of taking multiple samples, and maintaining said samples in isolation. Explored mechanisms included, but were not limited to: stored vacuum methods [98], capillary methods [99], piston and spring-based designs [21], and a rotary collection mechanism[95].

Rotary Sampling Mechanism

The sampling mechanism of the candidate device is based on rotary collection. The mechanism uses a motor-driven selector to expose and cover large reservoirs (sample chambers) prior to and following sample collection. Bulk transfer of material into the reservoirs is passive and relies on the muscular contractions of the GI in peristalsis. The pressures exerted by peristalsis can push thick, thixotropic, fluid into sampling chambers provided that the opening aperture is sufficiently wide[118,119]. These naturally occurring

contractile motions are leveraged to displace air and force luminal content into the sample chambers[120]. With this technique, the design challenge is simplified to keeping sampling chambers closed, exposing them at the appropriate locations, and closing once sampling is complete.

Three sampling chambers are evenly distributed around the longitudinal axis. In this configuration a single driving mechanism can independently expose and seal each chamber by rotating them in and out of alignment with the opening in the side of the device. The risk of cross-contamination is mitigated by: a) allowing sufficient time between successive samples for contaminant dispersal, and b) by minimizing the distance from the exterior to the chamber. Figure 1 illustrates the rotary sampling concept.

Having established rotary collection as the preferred sampling mechanism, a compact and powerful motor was required to align the sampling chambers with the sampling port. Pager motors, the micro DC motors used in cellphones or haptics for vibro-tactile feedback, were the appropriate size ranging between 2 – 6 mm in diameter and 15.8 – 20.8 mm in length. However, these motors were designed primarily to operate at speeds of 20,000-30,000 rpm and thus had to have their speeds reduced and torque increased using planetary gear attachments with reduction ratios of 70:1 to 500:1.

The motor is press-fit into the central hole of the sampling chamber body. For a more secure hold, the motor may be bonded to the sampling hardware with cyanoacrylate or other adhesive. In Embodiment A, the motor body is held stationary as the shaft rotates relative to the capsule. The shaft is coupled to the external shell with the sampling port. As the motor rotates, the sampling port is brought into and out of alignment with the sampling chambers. In Embodiment B, the shaft is held stationary as the motor body rotates. As the sampling chambers are directly coupled to the body of the motor, the recessed sections internally rotate into alignment with the sampling port. The consequences of a rotating motor body are increased stress on the PCB and a limitation of the number of revolutions due to twisting of its fixed leads.

During a typical course of device operation, the motor positions the sampling chamber six times (3 opening + 3 closing actuations). Extra capacity is provided in the event that

the device encounters small particulate occlusions. A 6mm (diameter) DC pager motor (Firgelli Automations, Surrey, BC, Canada) was selected for the candidate device.

Encoder for Rotational Positioning

Successful device operation is dependent on precise and reliable alignment of the sampling chambers with the sampling port. The pager motors selected for the embodiments of the candidate device lack position feedback and off-the-shelf encoders are poorly suited to this application due to size constraints. Direct contact, magnetic, and optical encoding were developed as custom solutions to obtain the appropriate form factor and resolution. They interface with the firmware in the same manner. Each transition causes an increment or decrement depending on the direction of rotation and the tally indicates the position of the sampling chambers with respect to the sampling aperture.

Hall effect sensing magnetic encoder

Magnetic encoding uses Hall effect sensors to detect the presence and/or strength of magnetic fields. A thin layer of plastic may be used to separate the sensor from the sampling area and prevent possible contact with fluid. The A3212EELLT-T (2x2x0.5mm) digital hall-effect sensor (Allegro Microsystems, Worcester, MA, USA) was selected for use in Embodiment A of the candidate device. This device outputs a digital low/high signal to the MCU indicating the presence/absence of a magnetic field.

Six cylindrical neodymium magnets, 1.5 mm diameter x 0.75 mm height (Plantraco, Saskatchewan), were embedded at 60° intervals around the base of the rotating sampling chamber section (Figure 10, inset A). The Hall-effect sensor detects a variable magnetic field as the motor drives the sampling chambers. The magnetic encoder is an effective solution however the presence of magnets within an ingestible device may raise safety concerns [121,122]. There is a risk that multiple ingested devices could magnetically attract one another and cause intestinal obstructions. For this reason, and for the purpose of minimizing the number of components, a third encoding method was implemented into Embodiment B avoiding the use of magnets completely.

Optical encoding

As with Hall effect sensing, optical encoding does not require direct contact with the rotating portion of the device. Optical encoding is based upon reflectance (transmittance) of light from (through) a given material. The encoding wheel may either block light intermittently or change the reflectance characteristics by having alternating sections with contrasting optical properties. Reflectance is preferred so that the source and receiver may be located on the same side of the encoder wheel. A commercially available infrared emitter-receiver pair performs this function. It is a 3.2 mm x 1.7 mm x 1.1 mm device with peak IR emission at 950nm and reception at 930nm. The sampling chamber is made from cast silicone polymer and has small protrusions at its base that intermittently block the IR receiver during rotation. Current flowing between the collector and emitter legs of the phototransistor is proportional to the photons received and generates a variable voltage as it flows across a 180Ω resistor. This voltage is read by the MCU's Analog-to-Digital Converter (ADC) to detect transitions.

3.3.2 Mechanical Design

Initial prototypes of the revolver concept were fabricated using a lathe and drill press. It was made from polycarbonate and had a single sampling chamber that went around nearly the entire circumference of the sampling chamber body. Subsequent prototypes were modeled in 3D CAD programs Alibre™ and Solidworks™ and possessed multiple chambers. The sampling chambers were exposed by being brought in- and out- of alignment with a large sampling aperture on the exterior of the device. Two embodiments of the revolver concept were designed: Embodiment A has its chambers remain stationary to the device as the sampling aperture was moved; Embodiment B has its sampling aperture remain stationary as the chambers rotated.

Device Enclosure (Embodiment A)

This device was designed around a ⌀6mm x 16.7mm, DC pager motor. It is comprised of three distinct components referred to as: Sampling Body, Selector Cap, and End Cap. The overall dimensions of this embodiment are ⌀11mm x 31 mm.

Selector Cap

The Selector Cap (Figure 10, inset A) is ⌀11mm x 16.5mm, fits over top the Sampling Body, and is held in place by the exposed motor shaft. This allows the Selector Cap to rotate freely over the Sampling Body. It has an inner diameter of 10.2 mm and a wall thickness of 0.4mm. The aperture in the side of the device is 9mm x 3.53mm. The anterior of the device has six recessed, ⌀1.5mm x 0.75mm, holsters evenly placed around the interior to hold D0100G N48 gold plated disc magnets (Gaussboys Supermagnets, Olympia, WA, USA). At the center is a ⌀2mm x 2.5mm socket or receptacle for the pager motor shaft.

End Cap

The End Cap (Figure 10, inset B) houses all electronics with the exception of the secondary PCB and the hall-effect sensor. It houses a bare-cell lithium-ion battery as well as an SPDT-NC magnetic switch. The End Cap is ⌀11mm x 14.5mm and also has a wall thickness of 0.5mm. It has three rectangular protrusions on its interior that interlock with grooves in the rear of the Sampling Body.

Sampling Body

The sampling body (Figure 10, inset C) is a ⌀10mm x 14.2mm cylinder with a 6mm hole in its center to accommodate a pager motor. Distributed evenly around its circumference are 3 sample chambers, each with 83.8μL capacity, as well as three ⌀0.8mm conduits to provide electrical connectivity at its anterior. The rear section of the sampling body bears L-shaped grooves that serve as a locking mechanism for the End Cap. Between each sample chamber opening is a non-recessed portion which seals the sampling aperture in the external Selector Cap. Unidirectional driving is sufficient in this embodiment for opening and closing chambers in series.

Device Enclosure (Embodiment B)

This embodiment differs from Embodiment A in the relative motion of its components, its rotational encoding mechanism, diversity of materials, and in its operational control. The overall design is larger at ⌀13.65mm x 34.96mm due to increased wall thickness and to accommodate a different mechanism in which the sampling chambers are rotated. It is designed around a ⌀6mm pager motor and consists of the Exterior Shell, Sampling Body, and the End Cap.

Exterior Shell

The exterior shell (Figure 11, inset A) is ⌀13.65mm x 29.46mm with wall thickness of 1mm. It is an enclosure for the sampling chambers, electronics, and power supply. A 2mm section at the rear of the shell has a decreased wall thickness of 0.425mm to accommodate the insertion of the End Cap. At the top of the Exterior Shell are pairs of holes for each sampling chamber. These are designed to accommodate 16 gauge needles used to extract the samples and aspirate the sample chamber. The Exterior Shell also bears a socket for the notched shaft of the pager motor.

Sampling Body

The Sampling Body (Figure 11, inset B) interfaces directly with the Exterior Shell and does not have any outer walls of its own. It has three recessed areas, which can store samples, and two non-recessed sections which block the sampling aperture in the Exterior Shell. Five small projections stand on the base of the Sampling Body to intermittently block the transmission of IR light during rotational motion. The device is 15.79mm long including the base projections and has an outer diameter of 11.7mm. The Sampling Body is coupled to the body of the ⌀6mm pager motor. The use of silicone improves the seal between sampling chambers as the rigid-soft seal compensates for small surface defects in the polycarbonate shell. Additionally, there is a double edge seal to isolate the electronics from intestinal fluid. The reduced number of blocking sections necessitates bidirectional motor rotation to maintain discrete sample collection.

End Cap

The End Cap (Figure 11, inset C) is a 7.5mm x 12mm (length x diameter) that seals all components into the device. It stores two coin cell batteries and fits into the end of the Exterior Shell. External IR communications occur through this polycarbonate piece.

3.3.3 Electrical Design

A microcontroller unit (MCU) integrates the functions of the medical device. With appropriate firmware it is able to time and control GI sampling. Bidirectional communication is also achieved with the MCU allowing the device to receive operating instructions and to transmit logged data. The MCU should feature: low power consumption, communication capabilities, and expansible ports to add features as required. It should operate over a range of voltages to avoid the need for "boost" circuitry (maintains a nominal voltage output despite dropping input voltage). The 8-Bit PIC12F1822/PIC16F1823 and the ATTiny84 MCUs from Microchip and ATMEL respectively were selected for development. These MCUs feature on-board multiple channel, 10-bit ADCs. Presently, the ADC is used for infrared communications and for positioning the sampling ports in line with the sampling aperture. In the future, pH sensing ISFETs could interface to the ADC to incorporate acidity trends along the GI for localization [79]. The electrical schematics and corresponding GERBER files were produced using EAGLE Electrical CAD software (CadSoft Computer GmbH, Pleiskirchen, Germany).

Electrical Schematic (Embodiment A)

The electrical schematic of Embodiment A consists of: a primary circuit (Figure 4) containing the IR phototransistor, magnetic switch, the MCU; and a secondary circuit (Figure 5) containing the magnetic Hall effect sensor and its supporting electronic components.

Microcontroller

The circuit is built around the PIC12LF1822 (Microchip Technology Inc., Chandler, AZ, USA) in an 8-VDFN package. This package has dimensions of 3x3x0.9 mm. It has 8 pins, of which 6 are programmable Input/Output lines (I/Os). The pins are able to directly

drive indicator LEDs or small peripheral devices with sink/source up to 25mA. It operates from 31kHz-32MHz on an internal oscillator and over a voltage range of 1.8 – 3.6V. The PIC12LF1822 features a 4-channel, 10-bit, internal Analog-to-Digital Converter (ADC) that may be used to read voltages generated at the leg of the IR phototransistor or from an analog variant of the Hall effect sensor. Additional sensors may also be attached to the unused analog-to-digital converter channels.

Communications Sub-circuit

A unidirectional communications system is implemented with a TEMT1020 IR NPN-Phototransistor (Vishay Intertechnology Inc, Shelton, CT, USA) and a 2.2 KΩ resistor. The phototransistor selected is compact with dimensions of 2.5x2.0x2.7 mm. Pin RA0, or 7 on the selected MCU package, is an ADC channel and is connected to the top of this resistor. As the phototransistor is exposed to infrared light (870-950nm), a cascade of electrons crosses the gate and generates a voltage that is read into the microcontroller through RA0 and interpreted in the firmware.

Motor Driver

One terminal of the motor is permanently connected to ground and the other terminal is connected to the output of a DG4157 SPDT Analog Switch (Vishay Intertechnology Inc, Shelton, CT, USA). A 1.00mm x 1.20mm x 0.55mm miniQFN6 package was selected. The use of this switch overcomes the MCU's current source/sink limitation of 25mA. It operates over a voltage range of 1.65-5.5V and is capable of handling 200mA continuously and peak currents of 400mA. The analog switch itself is connected directly to the power supply and is controlled by pin RA5 (pin 2 in the selected package).

Power Supply and Switch

The electrical circuit shows terminals for a power supply. Power is supplied to this circuit by a 3.7V 20mAh FR20 lithium polymer cell (Fullriver Battery Ltd, Guangzhou, China) similar to that used by Tortora et. al[45]. This battery cell has very high energy density. At 3.5 x 15.5 x 10mm and a weight of 0.8g it is able to discharge up to 20C (400mA), which is useful in the event that pager motor needs to draw higher current to overcome an

obstruction or initial static friction. The power supply is connected to the circuit through a commercially available Single Pole Double Throw, Normally Closed (SPDT - NC) magnetic reed switch rated for 500mA (continuous). A physical disconnect from the power supply maximizes device shelf life.

Magnetic Encoder Circuit

The magnetic encoder circuit is based on the A3212EELLT-T (2x2x0.5mm) digital hall-effect sensor (Allegro Microsystems, Worcester, MA, USA). A 50 KΩ pull-up resistor is placed between the device's output pin and the system voltage VCC (3.6V). A 0.1µF capacitor lies between the VCC and GND.

PCB Design (Rigid)

Separate PCBs were designed to accommodate the primary and secondary electrical circuits. Both are based on a rigid FR4 substrate and are unified with three wired connections (POWER, GROUND, SIGNAL) passed through dedicated conduits in the central portion of the device.

The secondary PCB, or the magnetic encoder, is a flat, annular, disc attached to the front of the sampling body. The primary PCB (Figure 14) is designed to fit into the horizontal plane of the device's rear enclosure. The front portion has solder connection joints to connect to the secondary PCB, as well as terminals underneath for In-Circuit programming and attaching the lithium polymer battery.

Electrical Schematic (Embodiment B)

Microcontroller

The electrical circuit for Embodiment B of the candidate gastrointestinal sampling device (Figure 7) is built around the AVR ATtiny84 (Atmel Corporation, San Jose, CA, USA) in a 20QFN package. It has 20 pins, of which 12 are programmable Input/Output lines (I/Os). It operates from 0-4MHz over a voltage range of 1.8 – 5.5V. Firmware is burned directly into the microcontroller unit (MCU) through the ISCP terminal indicated directly above the MCU in the schematic. The ATtiny features an 8-channel, 10-bit, internal

Analog-to-Digital Converter (ADC). Two of these channels are each connected to an infrared emitter-receiver pair. There also exists the option to attach a pH sensor, or some another sensor with analog output on any one of the unused analog-to-digital converter channels.

Communications and Encoder Sub-circuit

One infrared emitter-receiver pair serves as an optical encoder to determine the rotational position of the sample collection chambers with respect to the access port on the exterior enclosure. The other pair is used for external communication. The IR LEDs are driven directly by digital I/O pins on the microcontroller and are current limited to 18.3mA with a resistor value of 180Ω. A resistor value of 100㏀ is connected to the emitter leg of the phototransistor. This value creates a voltage output that can be directly fed to a digital input.

Motor Driver

The ATTiny84 can source 40 mA from each GPIO pin with a system maximum of 200 mA. However, the motor alone requires current exceeding 120 mA. This limitation is overcome through the use of a full-bridge motor driver which shares a common ground with, and is controlled by, the MCU but connects to a separate power supply – i.e. an independent silver oxide battery to prevent inadvertent system reset (brownout). The motor driver has two inputs connected to MCU pins PB2 and PA7 which correspond to pins 14 and 15 respectively in the 20QFN package.

Shunt Resistor

A 1Ω shunt resistor lies between one of the motor driver outputs and a leg of the motor terminal. It is a low-impedance resistor with high stability and low variation as its temperature increases. The shunt resistor allows current to be measured by the ADC channels on the MCU. Voltage fluctuations across the shunt resistor are translated into current values by dividing the measured voltage by its resistance. An ADC channel from the MCU is connected to either side of the shunt resistor allowing the MCU to detect the direction and current draw of the motor. Bidirectional capability is important for

releasing air bubbles from the sampling chambers as well as implementing the "wiggle escape" mechanism to release particulate matter.

Power Supply and Switch

The final subsection of the electrical schematic is the power supply and the master switch. Embodiment B utilizes coin-cell batteries which make better use of the space and shape of the capsule but require more complex electrical design. As with Embodiment A, the power supply is unregulated and the batteries are depleted during normal operation. Power is derived from two different chemistries: 1) Silver oxide battery and 2) Lithium ion battery for high and low discharge rates respectively. The high-discharge power supply is a 1.55V Renata 371 silver oxide coin cell battery (Renata SA, Itingen, Switzerland) permanently connected to the motor driver. The slow discharge power supply is a 3V, 30mAh, CR1025 lithium battery (Panasonic Corp, Osaka, Japan) connected to an SPDT-NC magnetic reed switch. Certain prototypes of Embodiment B utilize a commercially available solid-state switch, which in turn activates a high-current analog switch, DG4157 (Vishay Intertechnology Inc, Shelton, CT, USA).

PCB Design (Flexible)

The electrical circuit for Embodiment B was implemented on a flexible PCB to allow conformation to the cylindrical housing of the pill whilst allowing the protruding body of the motor to occupy the center of the cavity. The rectangular portion of the flexible circuit board (Figure 9) contains: ATTiny84 microcontroller, A3908 Motor Driver, Infrared Reflector Pair, motor terminals, passive components, as well as both the SPDT-NC magnetic reed switch and the MEMs solid-state magnetic switch.

The three circular sections of the PCB are battery terminals that fold in the manner illustrated in Figure 9. The rearward-most facing portion of the flexible PCB has an infrared emitter-receiver for external communication.

3.4 Firmware Design

Firmware for the device was written in C and MCU-specific assembly language. It is a state machine implemented through an interrupt service routine. The flowchart in Figure 8 outlines the operation of the firmware.

Communications

Firmware is programmed to the MCU following PCB population using contacts underneath the board. Once programmed, external communication occurs through a base station allowing operators to set run-time parameters: opening and closing times for each sample chamber, data collection rate, and mode of operation. Additionally, following transit, data logs may be downloaded to help with analysis of the collected samples.

In place of wireless RF communications or direct contact communications, infrared communications are used to communicate with the device. Infrared is well suited for this application as only short-range, line-of-sight communication is required. Prior to administration, the device communicates with a programming base station and/or computer through its translucent enclosure.

Embodiment A of the device utilizes a custom, unidirectional communication protocol. The communication protocol is based on the detection of variable-length LED pulses. Edge-detection is used to both count the LED pulses and time the duration of the pulses. Long pulses (200 ms) demarcate groups of data, and the sum of short pulses (50 ms) communicates an integer value. The data string consists of 12 integers that represent the hours (2 digits) and minutes (2 digits) at which each of the three sampling chambers should be exposed for sample collection. Infrared light fluctuations cause variable current through an IR sensitive phototransistor (Vishay Semiconductors TMT1020). This current flows across a 2.2 KΩ resistor on the emitter and produces a voltage detected by the microcontroller. The ADC is bypassed and the signal is sent directly to the sensing pin as a digital signal for increased speed and efficiency. Entry into the flowchart begins with the removal of the device's magnetic backing (activation). The MCU begins polling the receiver (Rx) pin connected to the phototransistor emitter. When a high voltage is read from the Rx pin the MCU begins searching for the START condition (initial long pulse).

A counter initiates to determine the signal length. The counter resets if the Rx reading transitions low before the START condition is met.

Embodiment B replaces the IR phototransistor (Vishay Semiconductors TMT1020) with a commercially available IR emitter receiver pair, which is used as a transmitter/receiver pair to implement Universal Synchronous/Asynchronous Receiving Transmitting communication protocol (USART, 9600 Baud Rate) between the device and the programming computer.

Device Activation and Programming

The device is activated with the removal of its magnetic backing at which point it checks for the presence of an infrared signal within a 5-second window. In this time period, it polls ATtiny84(PIC12F1822) pin PA2(RA0) attached to the output of the IR receiver. If a logical high input is detected, the device enters a communication mode in which it receives run-time parameters or offloads logged data. If no signal is received within this window then the device performs a search of the MCU EEPROM to determine its last state. In the event that the device has been previously programmed, the runtime parameters will be stored in the EEPROM as well as the progress of the program and the device will then resume operation from that location. Otherwise, if the EEPROM contains no information and an external signal is not being received, the device will enter a low-powered state until it is reactivated (application and removal of magnet) or powered-off. The parameters that are communicated to the device are: 1) the mode in which it is to operate; 2) the times at which to collect samples; and 3) the length of time that the chambers should remain open at each sampling location. Once the device has received its operating parameters it may be administered to the target recipient and enter the “main routine”.

Timing

Despite the various methods considered for positioning within the GI, time was selected for localization due to its simplicity and being required for future localization methods. The literature describes the transit time of the small intestine to be the least variable of

the digestive tract[104]. Initial animal tests would have the devices placed immediately beyond the pyloric sphincter, in which case a timing mechanism would be sufficient.

Timing is based on a resistor-capacitor (RC) circuit internal to the selected microcontroller. The operational frequency of the MCU is set to 1 MHz. The higher the speed of microcontroller operation, the more accurate the timer at the cost of increased power consumption.

A 30 second delay follows the successful programming of the device before starting the program clock to allow administration to the subject. A non-volatile system clock is implemented in the EEPROM that is updated every minute to minimize the writing cycles. Another counter is implemented in the volatile memory of the device which is incremented each twelve seconds when the device wakes from sleep. When this counter reaches five counts, the system counter in EEPROM is updated by one minute. Sampling times are limited to 1-minute resolution due to the EEPROM clock being used to compare the pre-programmed values.

Upon waking from sleep, the MCU (ATtiny84) pin PB0 is pulsed to blink the indicator LED. The system then checks the EEPROM system clock and compares the latest value to the programmed sampling (opening and closing) times. If the values match, the corresponding action is performed.

Sample Collection

The encoder is turned on and the MCU begins polling the SENSE pin. The hall-effect output signal is binary indicating the presence or absence of a magnet. The signal line is pulled up with a 50 KΩ resistor to VCC and is pulled to ground in the presence of a magnet. These correspond to logical High and Low signals respectively and require no further processing prior to being fed to the digital input - MCU pin RA0. With optical encoding, the signal is read by the ADC and compared to previous values. A pronounced shift in output will signal a transition.

The sampling chambers must be correctly positioned at the beginning of operation. This can be during assembly or manually positioned prior to operation. The encoder system

works by indexation with the initial position indexed to 0. Each transition detected by the hall-effect sensor when the motor is active increments or decrements the index for clockwise or counter-clockwise motion respectively. Through this indexation, the firmware keeps track of the sampling chambers relative to the sampling aperture as well as of its own progress in the sampling regiment. During sample collection, the sampling chambers are sequentially brought in line with the sampling aperture.

Motor Control

The duration of a transition is approximately two seconds. The device remains open until the system clock reaches the closure time-point. Following closure, the encoder and motor are deactivated and the MCU returns to its sleep state, waking every 12 seconds until the remaining conditions are reached or the program terminates. If two seconds of motor actuation pass without detection of a transition, then the duty cycle is increased to deliver more power to the motor. This is done by incrementing the existing value in the PWM duty cycle register by 10 until the maximum (255) is reached. Due to the heterogeneous nature of GI fluid, it is possible to encounter areas of increased resistance or particulate matter. In addition to increments in the power made available to the motor, an oscillatory motion is invoked to "wiggle" the motor back and forth to release blockages. At each stage of increased power, the motor is pulsed in the opposite direction momentarily and then remains stationary for 5 seconds to give the obstruction a chance to escape the chamber. After 5 seconds the motor is driven in its original direction until a transition is detected. If a transition is still undetected then the "wiggle" escape routine is attempted up to four more times before the system cuts all power to the motor and enters a sleep mode. The Interrupt Service Routine (ISR) is cancelled, a time stamp of the error is recorded in the EEPROM, and any future time-points are effectively aborted to preserve previously collected sample(s).

Pins PA7 and PB2 on the ATtiny84 and pin RA5 on the PIC12LF1822 are set as outputs and initiated to control the motor motion via the motor driver. Both MCU pins have Pulse-Width Modulation (PWM) capabilities used to control the power available to the motor in either direction. The program starts at a duty cycle of 60% (153/255) and increases it to 100% as necessary to overcome friction or obstructions. PWM is a means

of simulating analog output from a digital source by periodically turning on and off the source in pre-determined ratios. If performed at a sufficiently high frequency, the source appears continuous to the load. The motor control mechanism utilizes MCU *interrupts*, a means of executing select operations in the background, to allow the motor to be active whilst measurements and calculations are simultaneously performed.

Optional Current Measurement

A 1Ω shunt resistor lies in series with the load (motor). Measuring the voltage drop across this resistor provides a reading of the current being drawn by the load. ADC channels PA0 and PA1 take measurements on either side of the shunt to determine magnitude of current consumption and direction of motion – information which may be used to adjust PWM settings or simply logged. This feature was not utilized however, it is envisioned that future iterations will have motor control based on this feedback. This current draw will be used in determining the torque requirements of the motor and in adjusting the PWM routine of the motor in later stages.

Device and Sample Recovery

The device enters a low-power mode following program termination and continues to periodically (12 seconds) pulse an indicator LED making it more identifiable. If the power supply is not depleted, it may be reset by applying and removing a magnet in the presence of IR light followed by instructions to rapidly step through the same motions of sample collection so that samples may be scooped or aspirated from the chambers. In the event that the power is depleted upon recovery, the rear portion of the device may be removed to have power manually applied.

Power Management

Power consumption is minimized in the firmware by: reducing duty cycle, deactivating peripherals when possible, and making use of the microcontroller's "sleep" mode.

3.5 Results

Following numerous design iterations for the subcomponents of an ingestible sampling device, the efforts in this section resulted in the production of blueprints for two embodiments of a candidate gastrointestinal sampling device (Figure 13, Figure 12) and sources for off-the-shelf components required for its fabrication. These embodiments are ⌀11mm x 31 mm and ⌀13.65mm x 34.96mm in size respectively and embody the four critical subsystems required in a gastrointestinal sampling device: 1) system control implemented through custom-designed software and on-board MCUs, 2) a sampling mechanism based on a novel rotary collection mechanism and the muscular contractions of peristalsis, 3) a localization method using transit time as an initial metric, and 4) a power supply realized using batteries of various chemistries.

The mechanical components of both Embodiments A and B are designed such that they may be fabricated using rapid-prototyping technologies such as 3D printing in various materials. However, components of embodiment B were explicitly designed for fabrication from silicone rubber and polycarbonate using conventional subtractive machining techniques and/or thermoplastic injection moulding. Operational logic for the device was realized in 1200 lines of code and coupled to the mechanical components of the device with custom electronics and PCB designs. Collectively, these mechanical, electrical, and software designs should form a robust and capable gastrointestinal sampling device capable of collecting three discrete samples of 83.8 µL. The power management techniques incorporated into the firmware and electronics design result in an expected operational life exceeding 30 hours. In addition to the four critical subsystems, the resulting design possesses a means of communication to customize run-time parameters and to output logged data for retroactive analysis and further research.

3.6 Discussions

A number of gastrointestinal tract sampling capsules have previously been proposed in the literature [21,92,94,95,98,99]. Though each of these devices represent significant developments in the field of gastrointestinal sampling and possess important components required for capsular GI sampling, to date, none of the existing devices meet the criteria of non-invasively collecting and maintaining multiple heterogeneous samples from targeted locations in the GI for laboratory analysis.

In this section, selected components and concepts described in earlier devices have been integrated with a novel rotary sampling mechanism, communication system, and custom hardware and software to form the blueprints of a viable candidate device. Two embodiments of the candidate device were designed with slight variations to the sampling mechanism and electronics system. Embodiment A of the candidate device is designed for rapid prototyping using 3D printing whereas Embodiment B is designed for conventional manufacturing techniques such as injection molding.

The use of an MCU with an internal analog-to-digital converter for system control and the fact that the components of this design are integrated with software make this design of an ingestible sampling device inherently modular and thus suitable as a platform for many forms of gastrointestinal exploration and intervention. For instance, the sampling chambers could be modified to carry payloads such as medications, preservatives for collected samples, or antibodies for immunoassays without altering other aspects of the overall device design. These characteristics will facilitate continuous improvement and confer a level of versatility not available in current gastrointestinal exploration/intervention devices.

Further work is required to produce the candidate device from these designs and to evaluate and optimize its performance.

3.7 Acknowledgements

The author acknowledges Mark Drlik of Starfish Medical, Victoria BC, for his contributions to the mechanical design of Embodiment B.

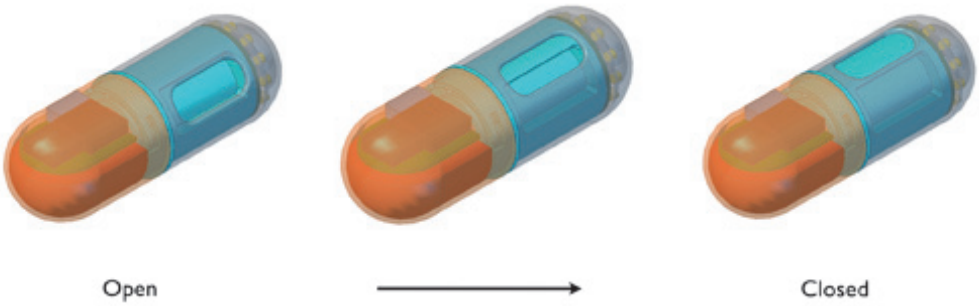

Figure 1: Illustration of basic rotary collection mechanism for GI sampling device

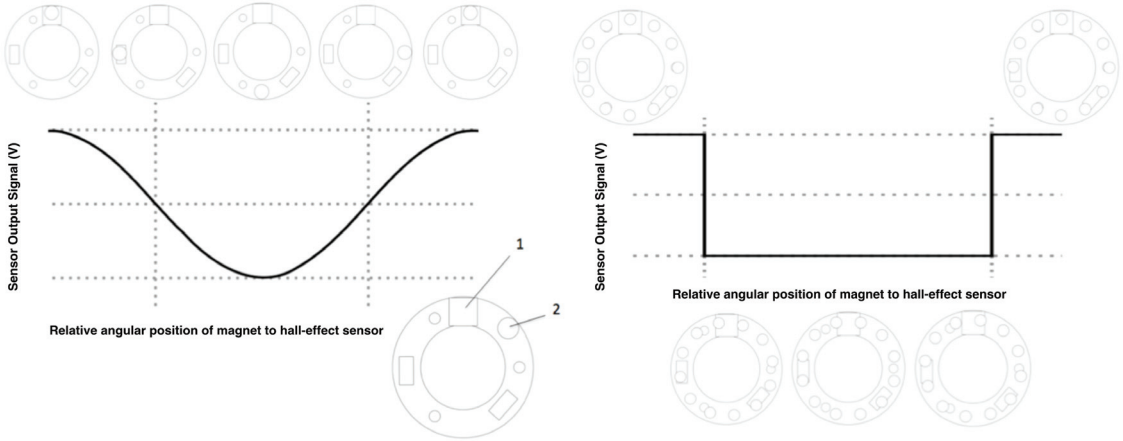

Figure 2: Theoretical output of Hall effect sensor (1) operating in analog (left) and digital (right) modes with rotation of the encoding magnet

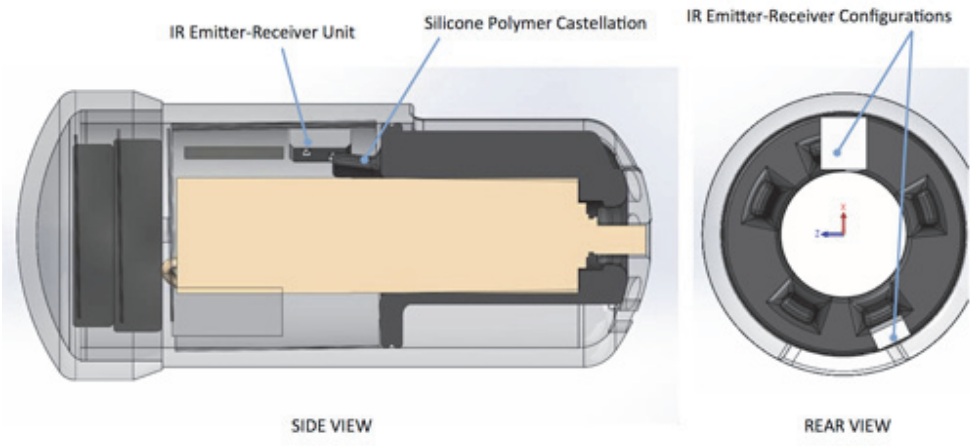

Figure 3: Configuration of silicone castellation with IR emitter-receiver pair to achieve optical encoding

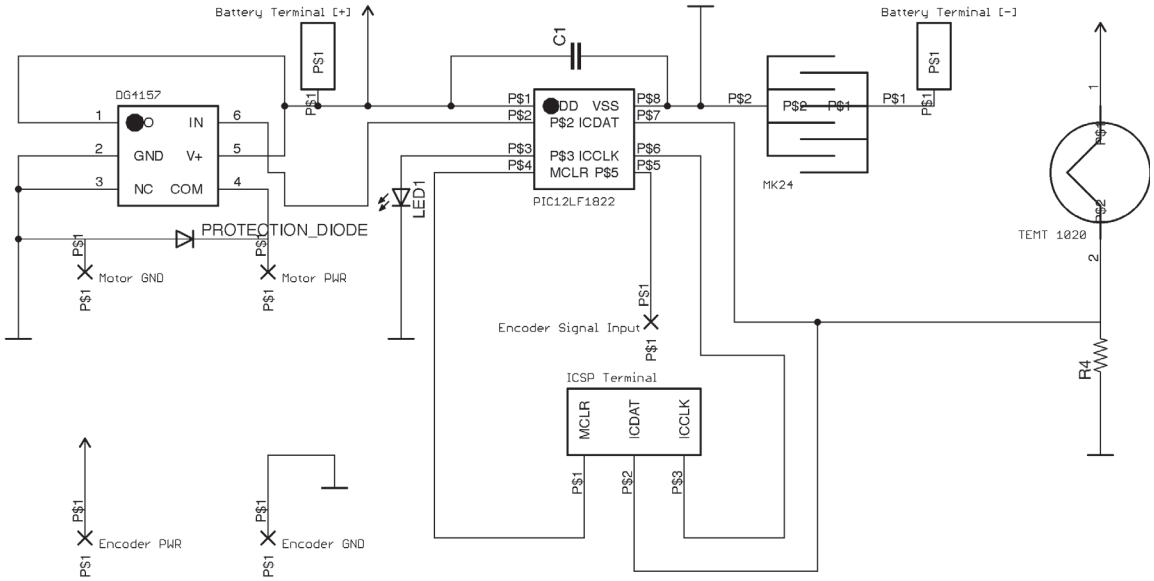

Figure 4: Electrical schematic of primary circuit (Embodiment A)

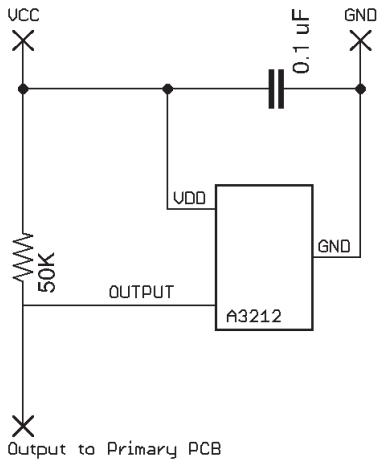

Figure 5: Electrical schematic of secondary/Hall effect encoder circuit (Embodiment A)

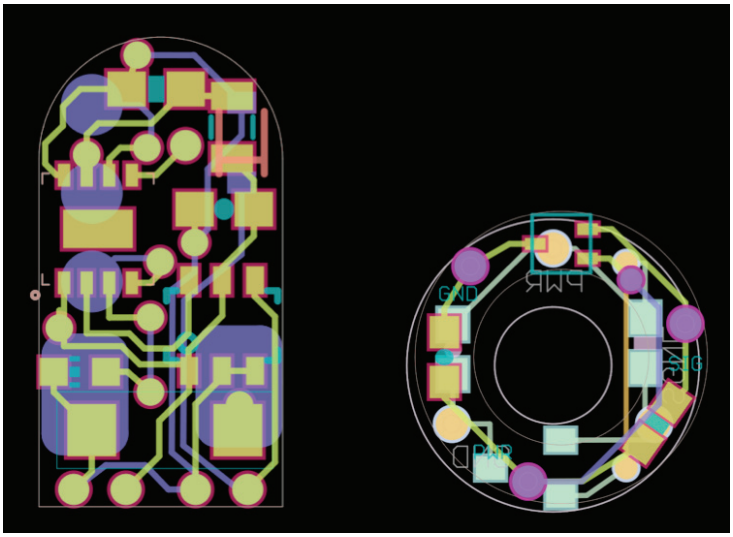

Figure 6: Component layout for Embodiment A primary (left) and secondary (right) rigid PCBs

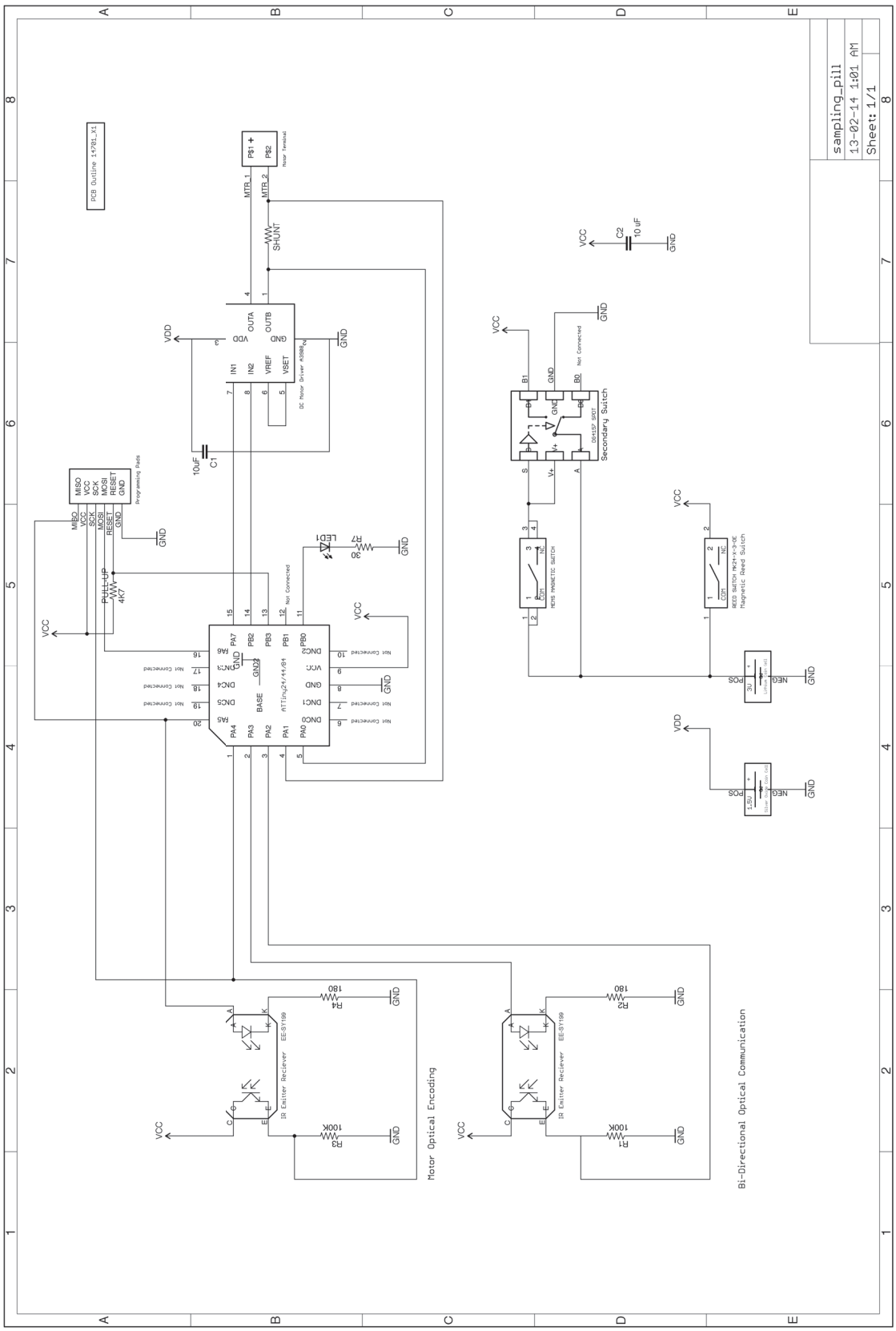

Figure 7: Electrical schematic of primary circuit (Embodiment B)

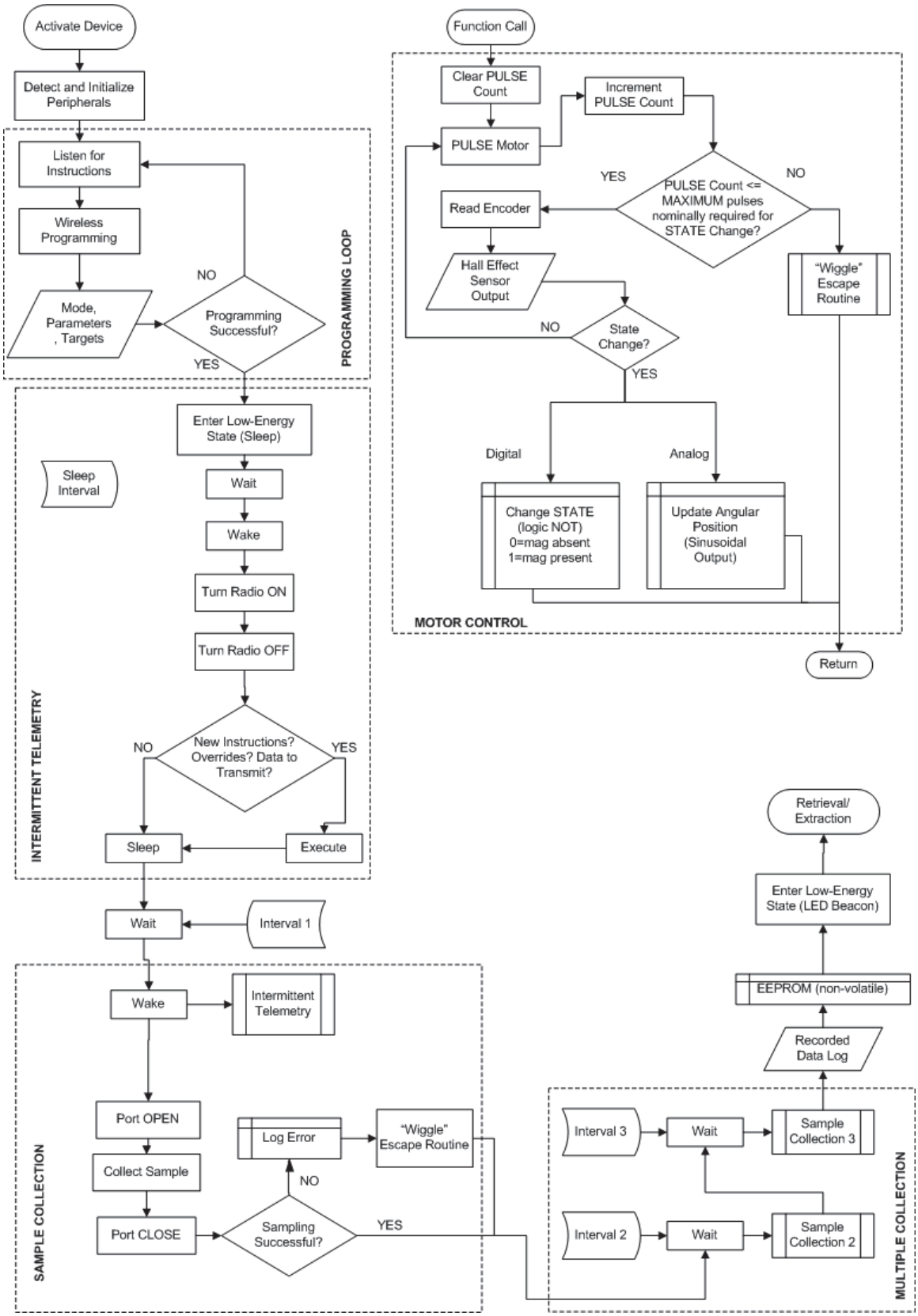

Figure 8: High-level flowchart for main program operation

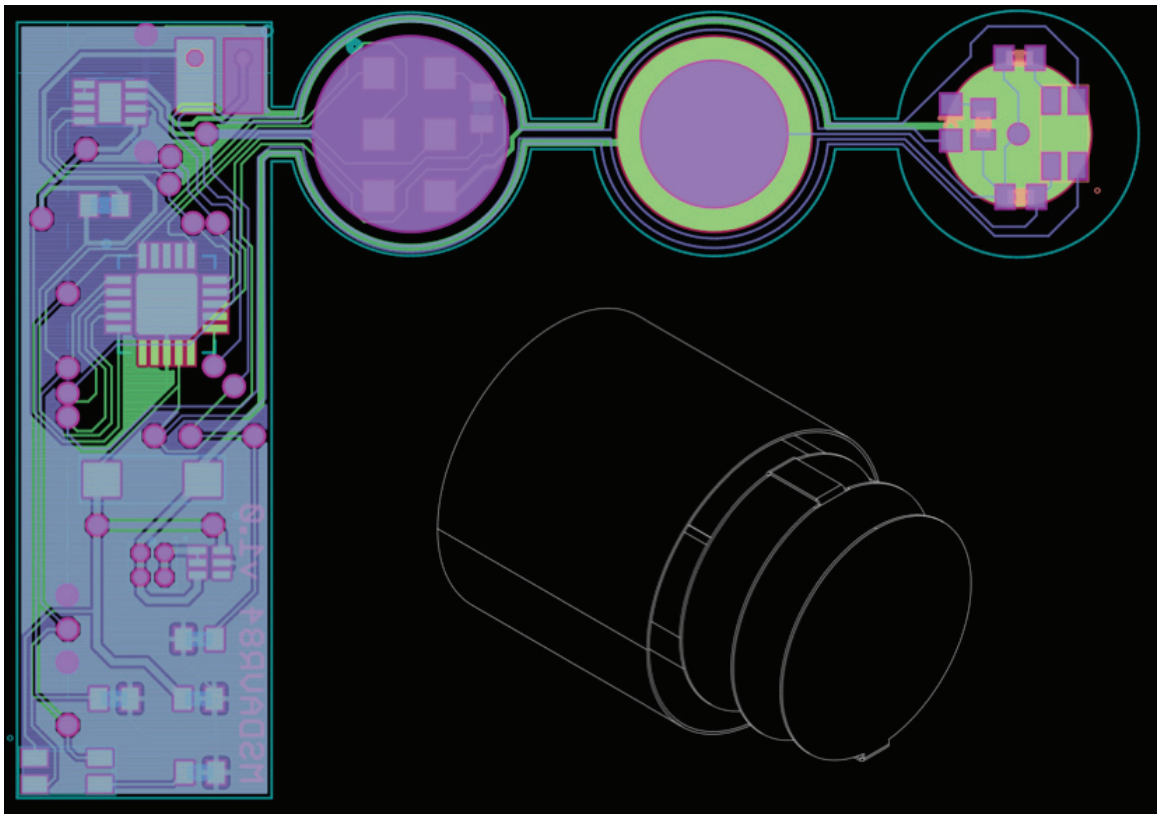

Figure 9: Flexible PCB layout and conformation (inset) for Embodiment B

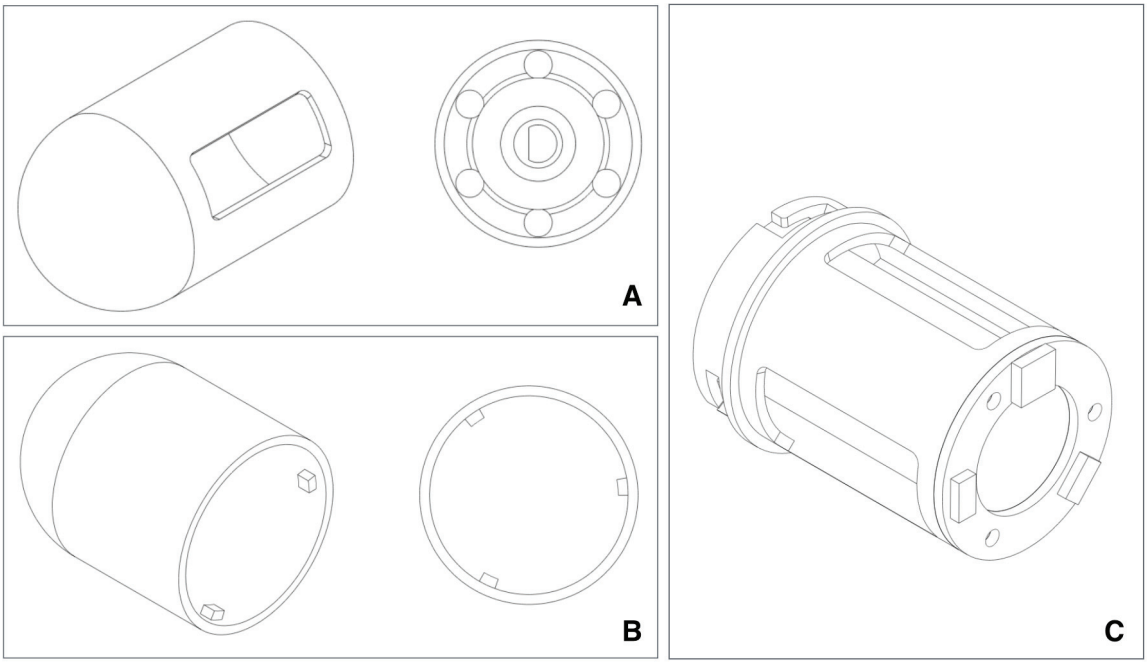

Figure 10: Mechanical design for Embodiment A selector cap (A), end cap (B) and sampling body (C)

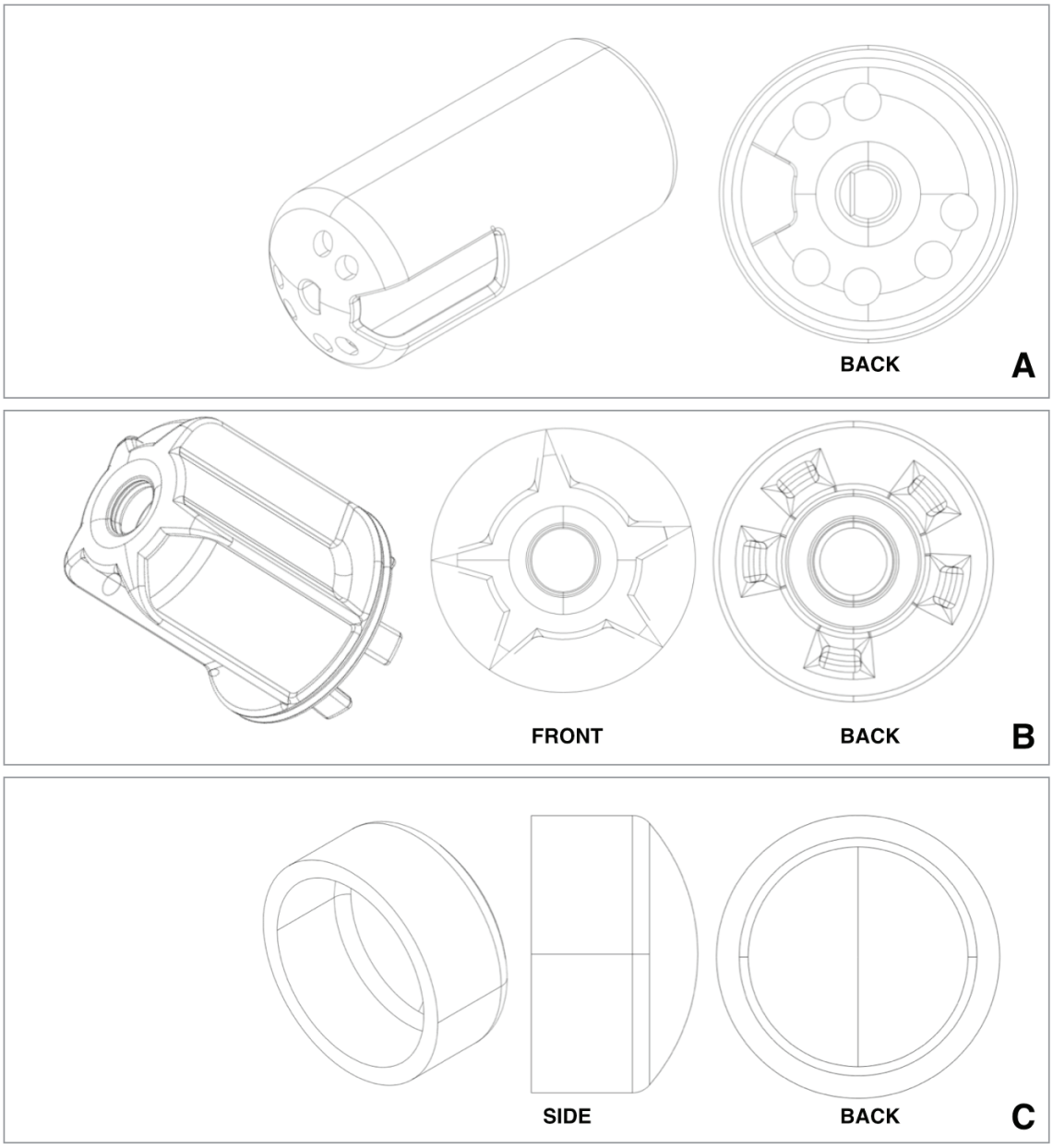

Figure 11: Mechanical design of Embodiment B Exterior shell (A), Sampling Body (B), and End Cap (C)

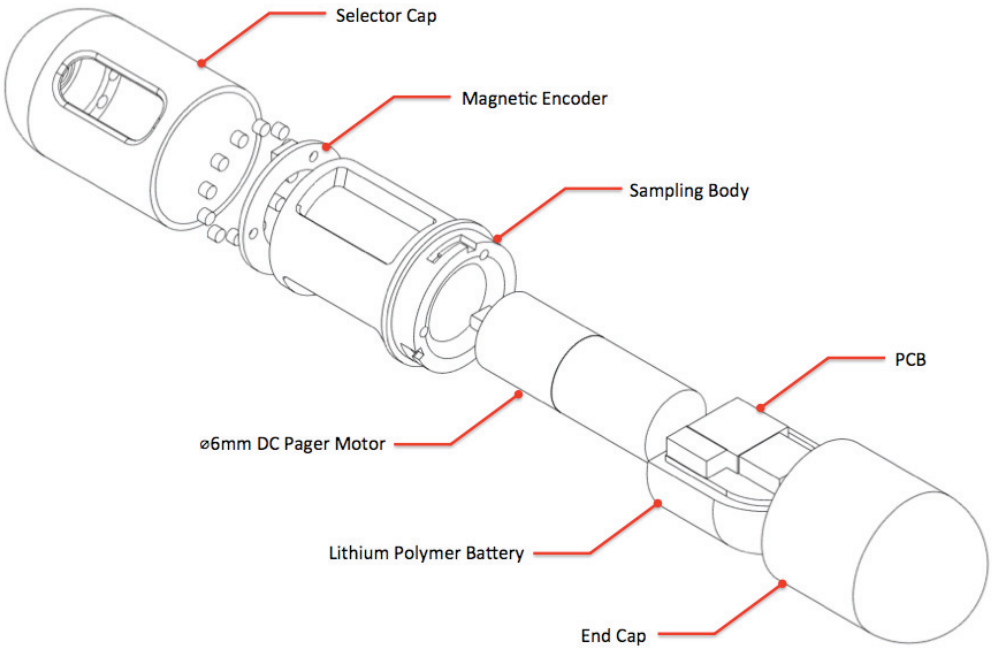

Figure 12: Exploded component view of GI sampling device (Embodiment A)

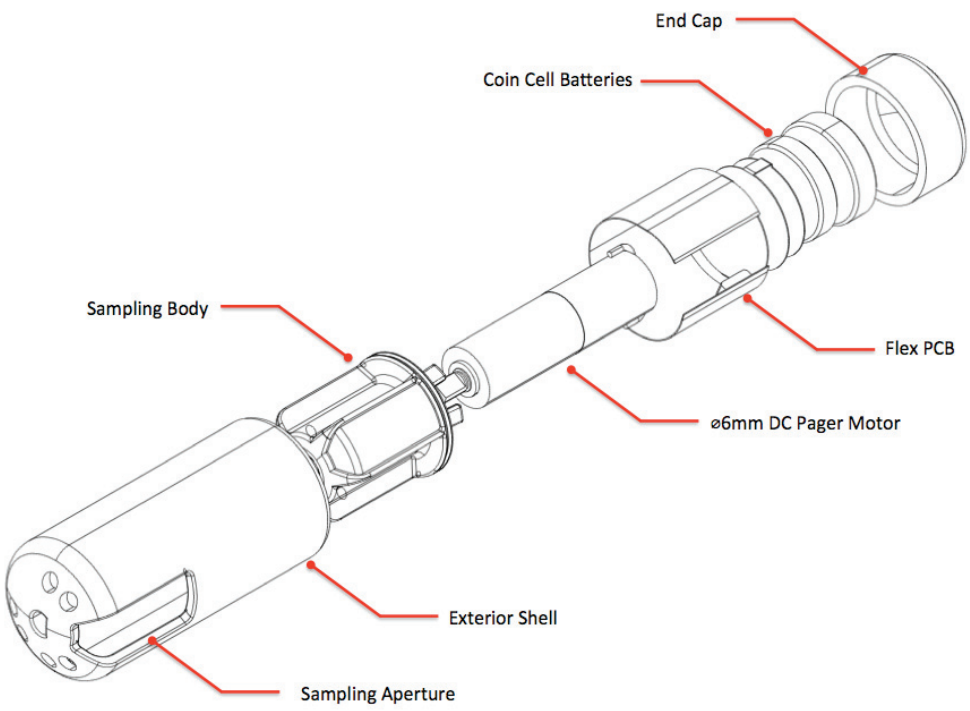

Figure 13: Exploded component view of GI sampling device (Embodiment B)

CHAPTER 4:

Subsystem Assessment and Optimization of an Electromechanical Gastrointestinal Sampling Device

Yaw Amoako-Tuffour, BEng [1], Mitchell L. Jones, MEng, MD, PhD[1,2], Alain Labbe, PhD[2†], and Satya Prakash, PhD[1,2]*

Biomedical Technology and Cell Therapy Research Laboratory

Department of Biomedical Engineering and Physiology

Artificial Cells and Organs Research Centre

Faculty of Medicine

McGill University

3775 University Street

Montreal, Quebec, H3A 2B4

Canada

---

[1] Biomedical Technology and Cell Therapy Research Laboratory, Dept. of Biomedical Engineering, Faculty of Medicine, McGill University, 3775 University Street, Montreal, Quebec, H3A2B4, Canada. Tel: 1-514-398-3676, Fax: 1-514-398-7461, Email: satya.prakash@mcgill.ca; mitchell.jones@mcgill.ca

[2] Micropharma Limited, 141 avenue du President Kennedy, UQAM, Biological Sciences Building, 5th Floor, Suite 5569, Montreal, Quebec, H2X3Y7, Canada. Tel.: 1-514-987-4151, Fax: 1-514-987-4616, Email: mitchell@micropharma.net; christopher@micropharma.net; satya@micropharma.net

* Corresponding author;

Key terms: medical device, ingestible capsule, gastrointestinal, sampling.

4 CHAPTER 4: Assessment and Optimization of Gastrointestinal Sampling Device Subsystems and Operational Performance

4.1 Abstract

The inability of existing gastrointestinal exploration methods to collect physical samples from the entirety of the gastrointestinal tract in a convenient, comfortable, and information-preserving manner prompted the specification of a new device possessing these capabilities. Prototypes of a previously designed electromechanical gastrointestinal sampling device were constructed and evaluated for subsystem integration and operational performance. The devices were assessed for: structural integrity using drop tests; ability to actuate in viscous liquid by means of water-glycerol solutions simulating the viscosity of the luminal fluid; ability to shear through partially digested matter; accurate timing and alignment of the sampling chambers with the sampling aperture; and in keeping collected samples free from contamination. The device successfully actuated in high-viscosity fluid with particulate matter; and was able to maintain three 40 mM solutions of GCA GDCA and TDCA in its chambers at 37°C for 12 hours with an average cross contamination level of 7.58%. The subsystems of the candidate device were able to perform to specification following: modifications to firmware enabling the device to withstand shocks, and unification of the power supplies to prevent motor-driver brownout.

4.2 Introduction

In gastrointestinal exploration and intervention, value is derived from being able to retrieve samples that are representative of the locations from which they were taken [22,63,67]. Collected samples become less representative of their origin with exposure to downstream contamination and degradation [123]. Cross-contamination is a concern with the sampling mechanism utilized in the candidate device as the samples pass through a common sampling port. Fluid migration between chambers as the device transits through the GI tract following sample collection may also occur. Significant levels of cross-contamination would compromise the integrity of the sample and necessitate design changes. The protocol of Jones et. al describing a method for bile acid determination by

HPLC, solutions of glycholic acid (GCA), taurodeoxycholic acid (TDCA), and glycodeoxycholic acid (GDCA), was used to assess levels of cross-contamination across the chambers [124]. Additionally, the device's ability to operate in viscous material and to shear partially digested food matter was assessed. Following a high-viscosity meal, the stomach quickly responds with intragastric dilution with shear rates falling from 11 Pa·S to 0.3 Pa·S after 30 minutes [125]. Therefore, a glycerol solution was used to simulate what could be considered a "worst-case" scenario for the device [126].

Fundamental to the operational performance of the gastrointestinal sampling device is the ability of its subsystems to properly interface with one another. Internally, firmware commands must translate into physical motions with the appropriate timing, positioning, and electrical characteristics. For overall operation, the capsule should be resilient to the forces and environmental conditions encountered during GI tract transit. The device may be susceptible to drops from table-height (1m) as well as to destructive mechanical forces in the GI of up to 2N [26,127]. The challenges encountered at each stage informed decisions in the device revisions.

4.3 Materials and Methods

Chemicals

Glycerol (MW 92.09, catalogue # G5516), Glycocholic acid hydrate (MW 465.62, catalogue # G2878), Glycochenodeoxycholic acid sodium salt (MW 471.61, catalogue # G0759), and Taurochenodeoxycholic acid sodium salt (MW 521.69, catalogue # T6261) were purchased from Sigma Chemicals (St. Louis MO, USA).

Method of Sampling Device Fabrication and Assembly

The 3-D models of Embodiment A and Embodiment B components were designed using Alibre® Design Expert 2011 (Geomagic, Richardson, TX, USA) and SolidWorks (Dassault Systèmes, Waltham, MA, USA), exported as .STL files and sent to manufacturers Shapeways (Netherlands) or Fineline Prototyping (Raleigh, NC, USA) to be printed. Electronic schematics and PCBs were designed with Eagle CAD software and the generated GERBER files were sent for manufacture at Gold Phoenix PCB (China).

In Embodiment B, 3D-Printing was used to create the mold for the Sampling Body which is made from a UV light-curable and medical-grade liquid silicone rubber (NuSil Technology, Carpinteria, CA, USA). The mold for this was drawn in SolidWorks and printed from a nickel-plated ceramic composite (Fineline Prototyping, USA). Biocompatible polycarbonate is used for the Exterior Shell of Embodiment B as well as the End Cap. A section of polycarbonate rod was turned-down on a conventional lathe prior to having the sampling aperture milled by CNC machine.

Upon receipt, printed components were washed with a solution of water and Hertel™ (Lavo Inc, Montréal, QC) and placed in a sonicator bath for 20 minutes to remove any remaining residue and particulate matter from the printing process. Following sonication, they are rinsed with water and dried with compressed air. Prior to circuit population, the Printed Circuit Boards (PCBs) are examined underneath a microscope to exclude defective pieces. It is common for PCBs such as these, with features and trace widths down to 4 mils (0.004”), to suffer connectivity issues (manufacturer quoted 15% defect rate in batch).

Once sorted, the boards were cleaned with metallurgical flux and had solder paste manually applied to the contacts. The ICs were positioned atop the solder paste before placing the PCB on a laboratory hotplate with digital read-out. Hot-plate temperature was ramped to 210°C over 1-2 minutes to reflow all components. A hot air gun was used to populate the flexible PCB (Figure 17). A basic LED-blinking program was loaded onto the populated boards to test functionality.

The pager motor was first inserted into the hole of the cylindrical sampling body. Six magnets (GuassBoys Supermagnets, Ridgefield, WA, USA) were then pressure-fit into the plastic selector cap. The annular PCB bearing the hall-effect sensor was carefully aligned with conduits going through the cylindrical body to supply power and to carry the sensing signal back to the main PCB. It is then adhered with superglue to the cylindrical body of sampling chambers.

Connections from the secondary PCB, the DC motor, and leads for the lithium polymer battery are soldered to the main PCB and a small sheet of silicone placed between the underside of the PCB and the battery to prevent shorting.

The selector cap is fit over the cylindrical sampling body and held in place by the motor shaft. After firmware has been programmed into the MCU memory, the rear end-cap is placed over the electronics and held in place by a locking mechanism built into the rear portion of the sampling chambers (Figure 15 insets: D, E).

In this embodiment the silicone sampling body was fixed to the body of the motor using an epoxy. The recessed shaft of the motor was inserted into a matching groove in the exterior polycarbonate shell.

Motor leads were carefully soldered to either side of the flexible PCB and the PCB inserted into the exterior shell with the IR emitter-receiver aligned with the wall of the sampling aperture. Batteries were attached using conductive silver epoxy (MG Chemicals, Surrey, BC) and cured overnight (12 hours).

Method of Operational Workflow (Firmware) for Sampling Device

Firmware was loaded onto the device using specialized programmers, the PICkit 3 PG164130 (Microchip Technology Inc., Chandler, AZ, USA) and the AVRISP MKII (Atmel Corporation, San Jose, CA, USA).

Early prototypes of the first embodiment used PDV-9200 photocells (Advanced Photonix Inc, Ann Arbor, MI, USA) sensitive to 400-700nm wavelengths for communication. These were replaced with the TEMT1020 IR NPN-Phototransistor (Vishay Intertechnology Inc, Shelton, CT, USA) and an infrared emitter-receiver pair to overcome ambient light interference. Run-time parameters may be set on the device through these opto-sensors. An Arduino™ Uno (Sparkfun Electronics, Boulder, CO, USA) is used to drive a single IR LED or an IR emitter-receiver pair and to interface with a computer. Through the Arduino™ and its serial interface, the desired sampling times are transmitted using either a custom protocol or standard UART.

For testing purposes, all wait times and actuations were placed at one-minute intervals. Following run-time parameter programming, the device immediately begins stepping through the program. Accurate transitions indicate successful communication/programming and program execution.

Embodiment A possesses three recessed sampling chambers alternating with three non-recessed sections and operates with unidirectional motion. Embodiment B operates in a similar principle but requires bidirectional motion due to the elimination of one non-recessed/blocking such that the remaining two blocking sections may be reused. The firmware command *forward()* corresponds to counter-clockwise movement of the sampling chambers and *reverse()* translates to clockwise motion relative to the exterior shell.

In Figure 20, the black arc represents the aperture exposing the recessed area to the contents of the GI. In its initial position, A, a non-recessed section blocks the port. The sampling chambers then rotate one position counter clockwise to position B, exposing the first recess to the port. The sampling chambers proceed to move clockwise incrementally alternating between open and close states. There is a reversal at the final step (F) where the juicer must return to the previous block to avoid re-exposing the adjacent recessed section. In general, the sampling body may have N number of chambers and N-1 number of areas that are not recessed separating the chambers. The storage sub-unit may rotate in the second direction for a predetermined number of stages as described by the following formula.

$$\#\text{ of Positions in Second Direction} = 2 \times (N-1) \qquad (1)$$

Where *N* is the number of chambers in the storage sub-unit before the storage sub-unit again rotates in the first direction to complete the collection and/or release operation.

Method of Assessing Accuracy of Sample Chamber Rotational Positioning

Device functionality is dependent on the ability to accurately align the sampling chambers. This is required to seal the collected samples against external contamination.

Alignment was assessed by measuring the edge-to-edge distance between the sampling chamber and sampling aperture wall.

Method of Determining Power Consumption of Candidate Sampling Device

The largest power consumers in the device are the motor, microcontroller, and motor driver in descending order. At a voltage of 1.5 V the motor draws up to 150 mA from the silver oxide battery. However, the motor need only be actuated six times during the entire assay for a total duration of approximately 12 seconds. The power consumption is determined with in-line measurements of current flow between two test terminals at known voltage on the PCB. This was performed in both its low-power "sleep-state" and high power "wake-state".

Method of Assessing Structural Resilience of Capsule to Mechanical Shock

The assembled device was dropped from a height of 1m to assess resilience to damage from an inadvertent tabletop drop. With a weight of 5.01g for the device, the force of impact was equal to 50mN. Structural damage to the device exterior was assessed qualitatively whereas internal damage was indicated by a stoppage of program execution.

Method of Evaluating Impact of Viscosity and Particulate Matter on Device Actuation

A candidate device was placed in 100% wt glycerol elevated to 37°C in a water bath (382.4 mPa·S) to determine the operability of the device's sampling mechanism [126]. Moderately cooked pasta was also placed within the sampling aperture to be representative of particulate matter and partially digested foods that would be encountered in normal operation. Revolutions of the sampling chamber were timed at 100 % wt glycerol and 50% wt glycerol aqueous solution to identify appropriate actuation times for the firmware.

Method of Evaluating Cross-Chamber Contamination in GI Sampling Device

Three 40mL solutions of 50mM GCA, TDCA, and GDCA were made and placed in a plastic tray. The sampling devices were sequentially submerged in each of the baths for 5 minutes, closed, washed in a distilled water bath for 30 seconds, and then submerged and

opened in the next bath of Bile Salt Hydrolases (BSH) (GCA, TDCA, and GDCA respectively). Following sample collection, the devices were placed in an incubator and stored at a temperature of 37 °C. This process was repeated for an incubation period of 1 hour, 2 hours, and 12 hours. Following the incubation, the liquid was extracted from the chambers using two 25 Gauge needles – one to aspirate and extract the sample and the other to equalize the pressure within the chamber. The extracted samples were analyzed in an HPLC machine using a previously established protocol[124].

4.4 Results

Subsystem evaluation resulted in several modifications to the device design. Embodiment B of the candidate device experienced severe brownouts when it was powered by its internal supply instead of a bench-top power supply and made to drive the motor. This was due to an incompatibility of the motor driver with the electrical design of the device. The selected full-bridge motor driver has a single power input for powering both itself and its load instead of segregated sources. With each signal form the MCU to apply power to the motor, the lithium battery voltage would drop to 1.8V due to the current draw and result in a brownout of the driver IC as this voltage fell below the minimum 2V threshold. The problem is addressed by doubling the voltage sensed by the motor driver without increasing the dimensions due to fixed distance between battery contacts, or by replacing the motor driver with one with segregated inputs such as a high-current analog SPDT switch (require a pair to maintain bidirectional motion). The latter option requires a board redesign. In the short-term, the issue was addressed by modifying the existing PCBs to merge the independent power supplies. The modification (Figure 21) consisted of two steps: 1) a bridge was created between the front and rear of the central battery contact. 2) The trace connecting the top battery to ground is severed. The result is a transformation of a power system consisting of two isolated batteries, into a supply based on two batteries in series. The lithium battery was replaced with another silver oxide battery for cohesive discharge characteristics. For majority of operation, the logic circuit operates at 3.10 V (1.55 + 1.55 V). When the motor is actuated a voltage drop of 1V can occur without affecting operation because the MCU is functional down to 1.8V and the motor driver is able to power the motor without experiencing brownout.

Prototypes printed from UV-light curable acrylic polymer were quite brittle as an artifact of the 3D printing process. However, exterior housings machined from solid polycarbonate were able to withstand the drop test. This test revealed that the aspect of the design most vulnerable to disruption was internal. The main power switch is a compact, normally closed, magnetic reed switch. Contact may be broken with magnetic fields or mechanical shock. In the firmware developed prior to this test, such a disruption in the power supply would reset the device and the program would restart. In response, changes were made to the firmware allowing it to store time and current conditions in the non-volatile memory of the MCU (EEPROM). At the entry point to the program, a condition was added to distinguish between an intentional reset and one caused by shock or brown-out: The MCU searches for an IR signal by reading the voltage level on its ADC channel 2. If no signal is detected within 1 second, then it is interpreted as a soft reset or brown out. The MCU then resumes the program by loading in the last conditions stored in the EEPROM.

Rotational positioning tests revealed occasional misalignment by 0.5-1.0mm. Fortunately, misalignment is a non-accumulating error. Because the occurrence and severity of misalignment are independent of errors in previous positioning steps, correction is achieved by modifying the 3D model of the external enclosure to reduce the width of the sampling aperture and create a 1mm overlap with the sampling chambers.

At 3V the microcontroller consumes 0.4 mA (Sleep) to 1.3 mA (Active) of current. Firmware was based on a 12 second interrupt driven by a 16-bit timer. Every 12 seconds, the microcontroller woke from sleep to check its status and to pulse the indicator LED. If any sampling conditions were met, the motor and encoder were activated and sample collection initiated. During the intermittent sleep periods, when only the 16-bit timer was functional, the current consumption is at its minimum 0.4 mA. When active, the current consumption could reach 1.3 mA due to the LED being directly driven by the MCU. Finally, the A3908 motor driver (Allegro Microsystems, Worcester, MA, USA) draws an additional 0.500 mA from the primary power supply when active. Based on Renata 371 (Renata SA, Itingen, Switzerland), 40mAh, silver oxide coin cell batteries, the expected lifespan of the device is between 27 and 30 hours.

Sample Collection of Viscous and Particulate Containing Fluid (Shearing)

The revolving portion of the device was able to turn unimpeded in the simulated conditions and the sampling aperture was sufficiently large to be passively filled by the fluid. There was however, significant decrease in actuation velocity with increased viscosity illustrated by the rise in revolution time from 4.62 s in 50% weight glycerol solution to 10.70 s in 100% glycerol (Figure 25). Air bubbles became trapped in the fluid, however these are able to escape with sufficient exposure and movement from simulated muscular contractions.

Embodiment B, with its sampling ports extending to the front of the device, is the preferred solution. In practice, content enters from the front of the device as it advances with peristaltic motion. It remains important to have side access for air release and to capture samples of the bacterial populations residing on the walls of the GI. The device was able to collect sufficient sample (>80% of the sampling capacity). It was demonstrated that: heterogeneous sample can be collected from the lumen using the revolver mechanism.

Inter-chamber Cross Contamination

HPLC analysis revealed a low level of cross contamination between the chambers. Figure 26 indicates the composition of the recovered samples from the chamber. With zero cross-contamination, chambers A, B, and C would contain 100% GCA, TDCA, and GDCA respectively.

The 2-hour trial had significant error introduced due to mishandling of the external polycarbonate shell. The 2-hour time point was disrupted due to upward movement of the polycarbonate shell on the aluminum base creating space for samples to migrate across chambers. Excluding the 2-hour time point, the results indicate that the rotating mechanism, achieves low and consistent levels of cross-contamination to warrant continuing research. The upper limit is 12.76% contamination and the average across the 1 hour and 12 hour samples is 7.58%. The low-viscosity samples were able to seep through surface imperfections and into the adjacent chambers. It is presumed that, all else being equal, samples of higher viscosity (such as those in the gastrointestinal tract) will

be less likely to bridge these imperfections and show lower levels of cross contamination. The results from the cross contamination indicate an upper threshold that is not exceeded with increased time. The degree of contamination and the relative composition of the contaminants across chambers are nearly identical at the 1-hour and 12 hour time-points. This suggests that cross-contamination is independent of time after 1 hour and instead largely dependent on the physical design of the device. This may be improved by a finer machining of the surfaces and further adjustments to the shape of the sampling chambers.

4.5 Discussions

The designs for the mechanical, electrical, and software subsystems of an autonomous gastrointestinal sampling capsule were previously developed. In this section, these designs were realized in the fabrication of prototypes. The subsystems of these prototypes were evaluated for their ability to perform to specification and for proper integration with one another. As a result of testing, the design was optimized in various areas including: at the software level to improve fault tolerance (i.e. resistance to shocks), and within the electrical system to resist/prevent brownouts. With these changes, the subsystems were made fully functional. Further testing validated the novel sampling mechanism as being capable of: capturing physical samples in simulated conditions and maintaining them as discrete samples with low cross contamination levels until their due recovery. Ongoing evaluation and optimization will occur with Embodiment B of the sampling device due to its simplified component design and its resilience to structural damage as demonstrated in this section.

Future developments include mechanisms for device retrieval following GI tract transit and the investigation of methods for halting enzymatic and chemical processes through quenching additives or temperature treatments. An appropriate animal model must be selected for further in-vivo safety and performance studies prior to clinical tests in humans.

4.6 Acknowledgements

The author acknowledges the contributions from Mark Drlik and Christian Proch-McMechan of Starfish Medical for the fabrication of the silicone sampling chambers. The

author acknowledges the contribution of Hongmei Chen for her work with the HPLC analysis and with the preparation of the bile salt solutions.

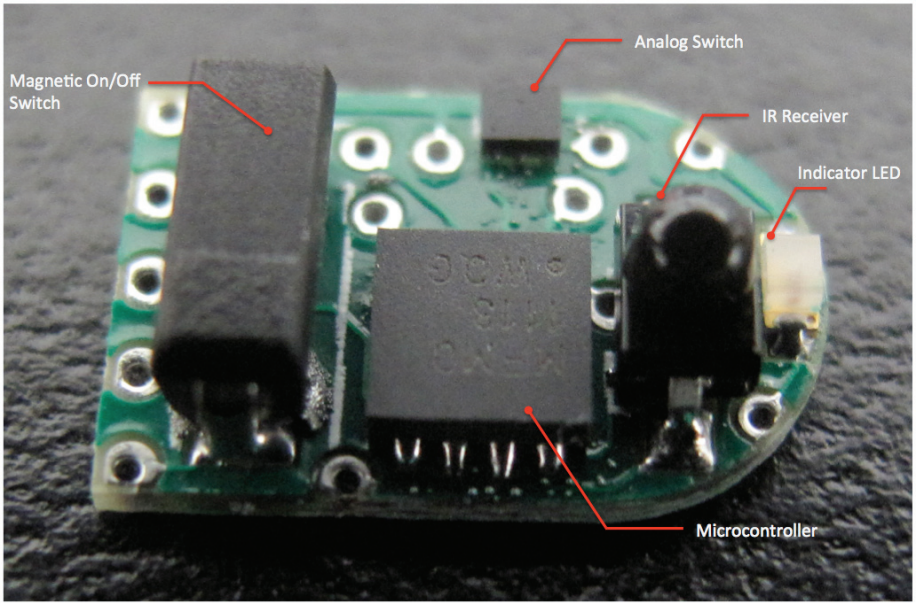

Figure 14: Rigid PCB of Embodiment A primary circuit populated with IC components

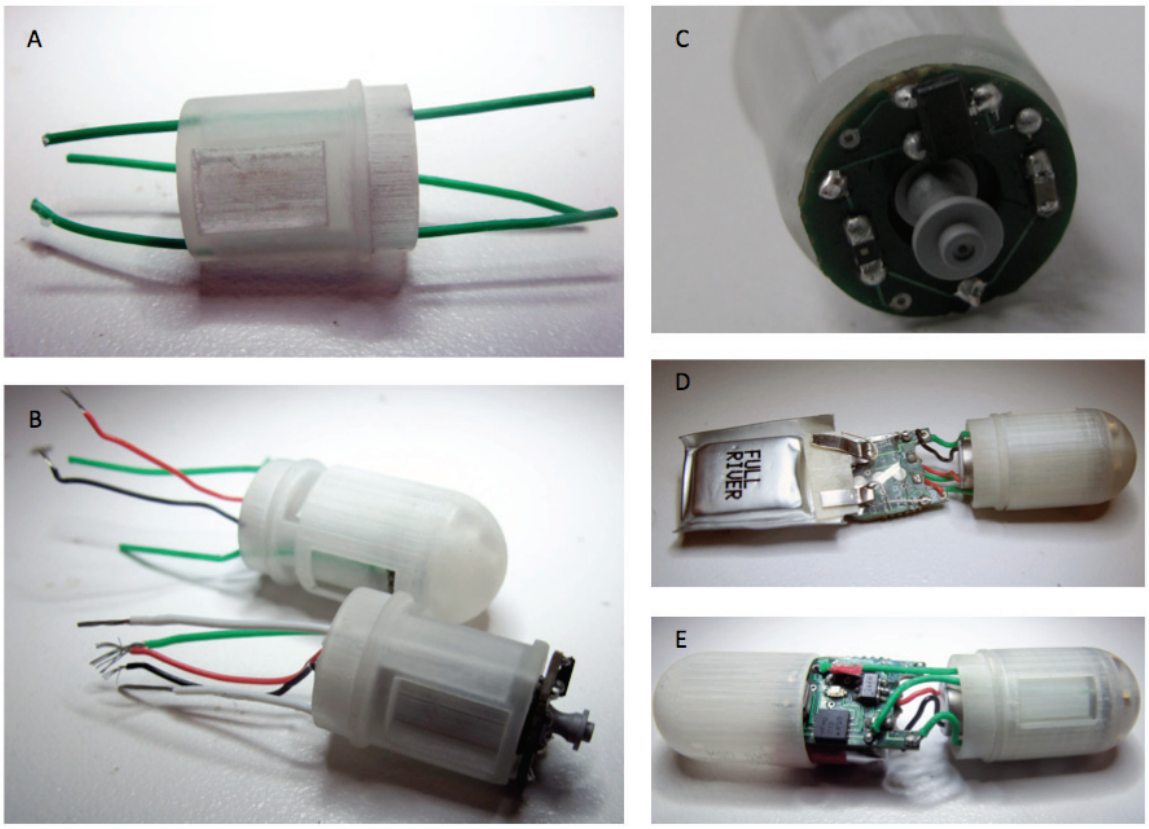

Figure 15: Assembly of GI sampling device (Embodiment A) a) insertion of wires into the sampling body conduits, b) fitting of motor into central portion c) attachment of magnetic encoder annular PCB d) magnet fitting and battery connection e) external shell assembly

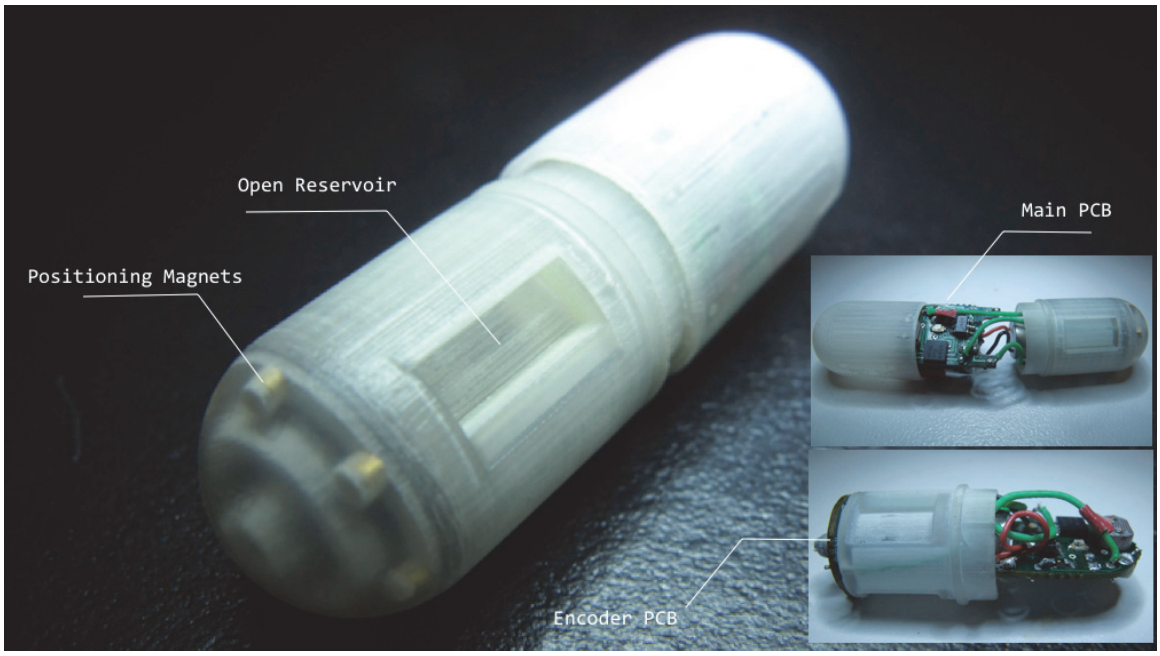

Figure 16: Embodiment A prototype fully assembled, and in various stages of assembly (inset)

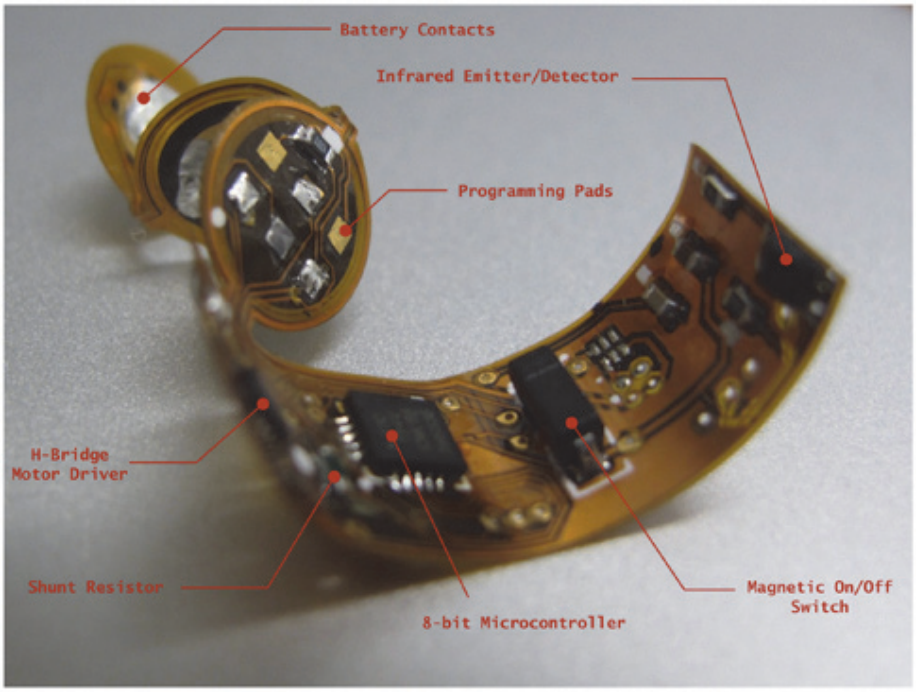

Figure 17: Populated and partially conformed flexible PCB

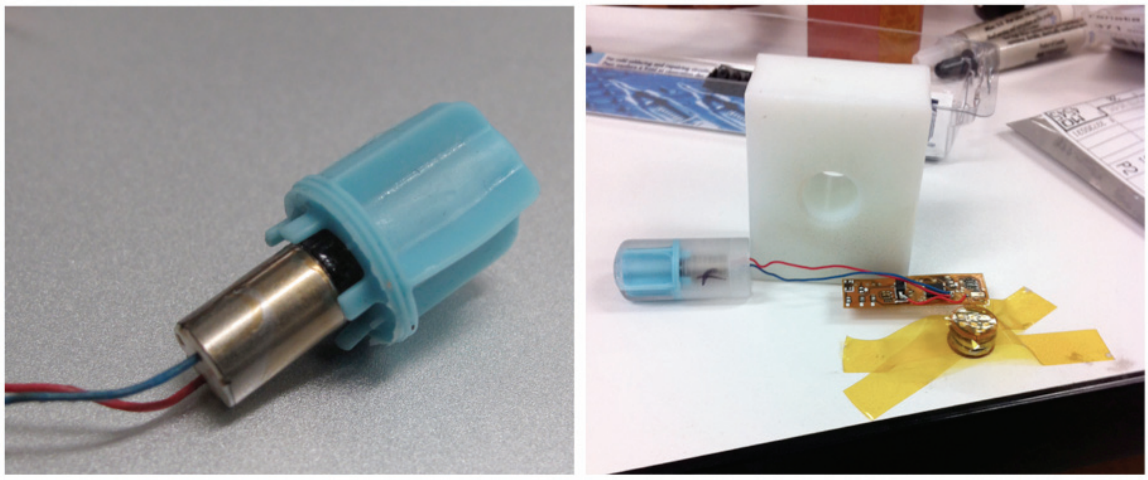

Figure 18: Assembly of sampling device (Embodiment B) with a silicone sampling chamber epoxied to motor body (left) and a silver-oxide battery stack held with conductive silver epoxy (right)

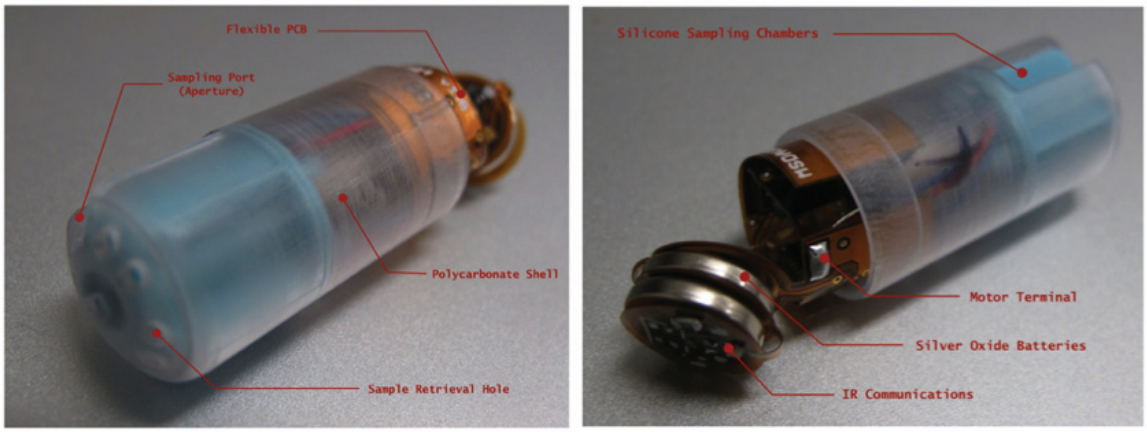

Figure 19: Assembled prototype of GI sampling device (Embodiment B) with internal components exposed - front view (left), and rear view (right)

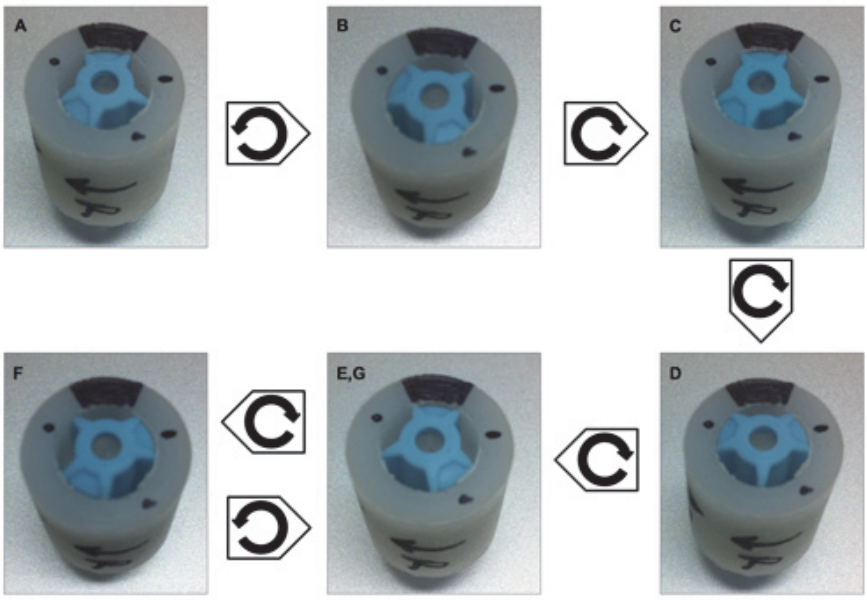

Figure 20: Bidirectional sample collection movements with 'A' and 'G' indicating initial and final positions and black arc representing the sampling port

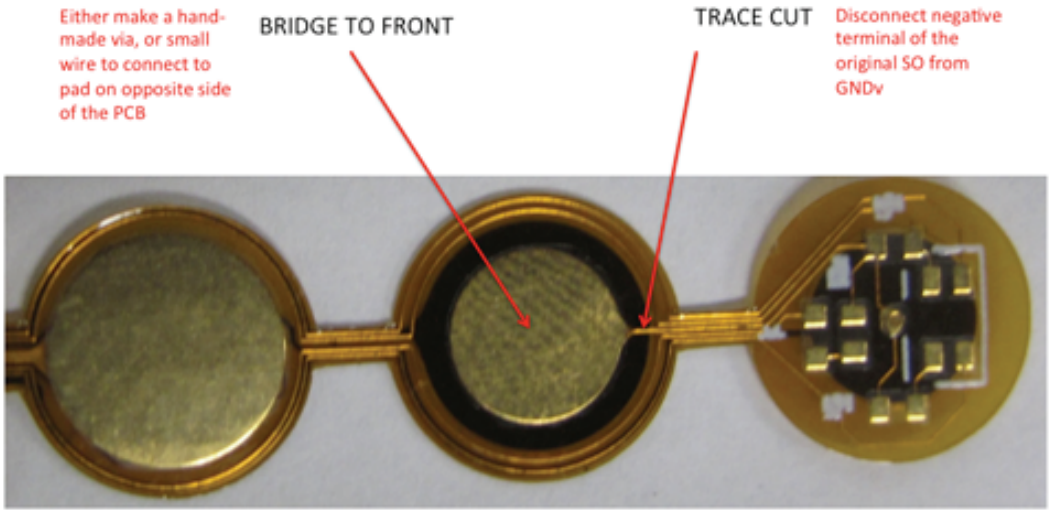

Figure 21: Board modifications to flexible PCB to serialize previously independent power supplies

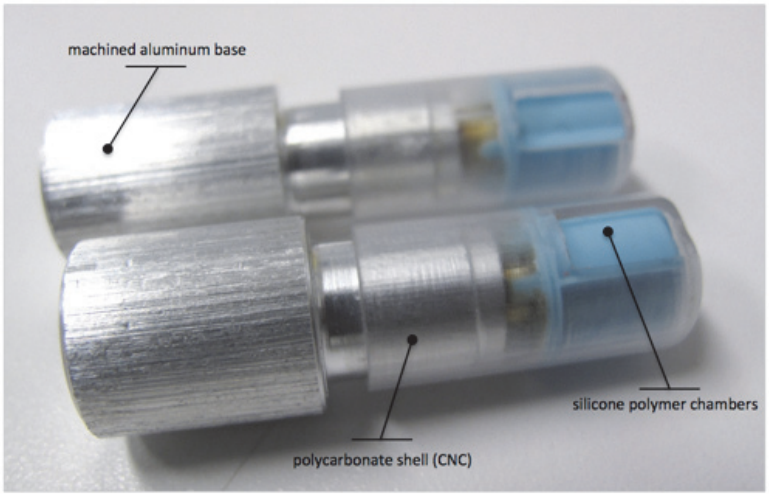

Figure 22: Aluminum based testing devices for cross-contamination evaluation of rotary collection mechanism

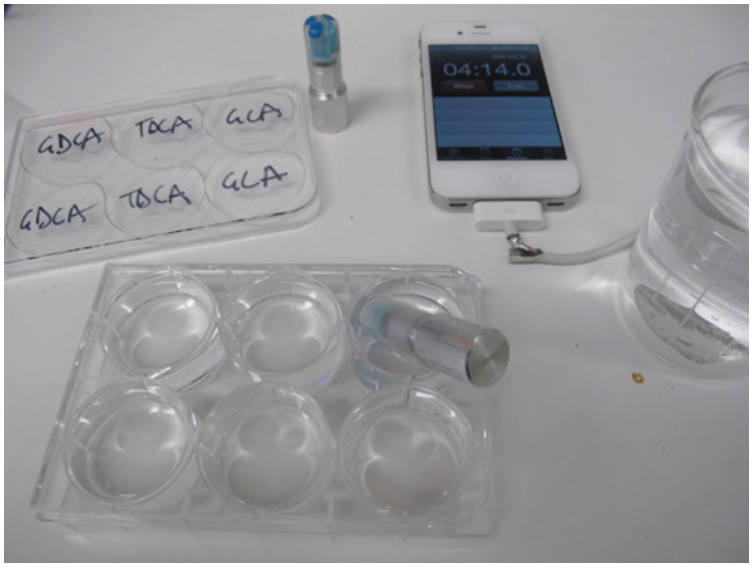

Figure 23: Series of wells containing GDCA, TDCA, and GCA for inter-chamber cross-contamination in candidate GI sampling device

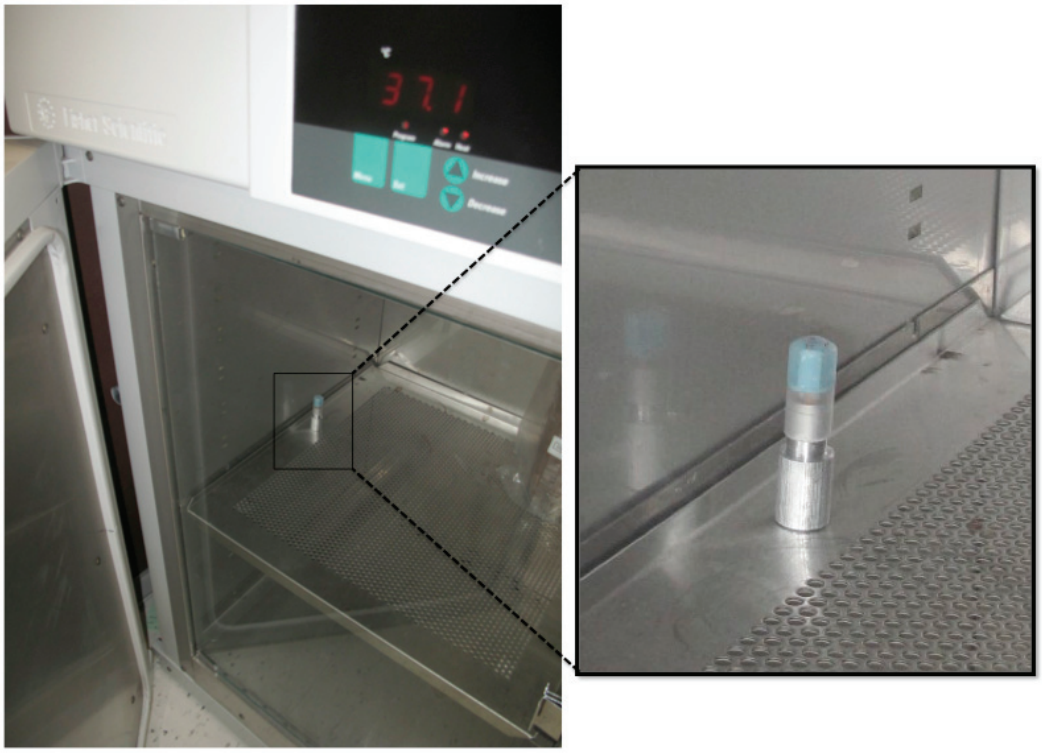

Figure 24: Sampling device placed in incubator at 37 degrees Celsius for 12 hours

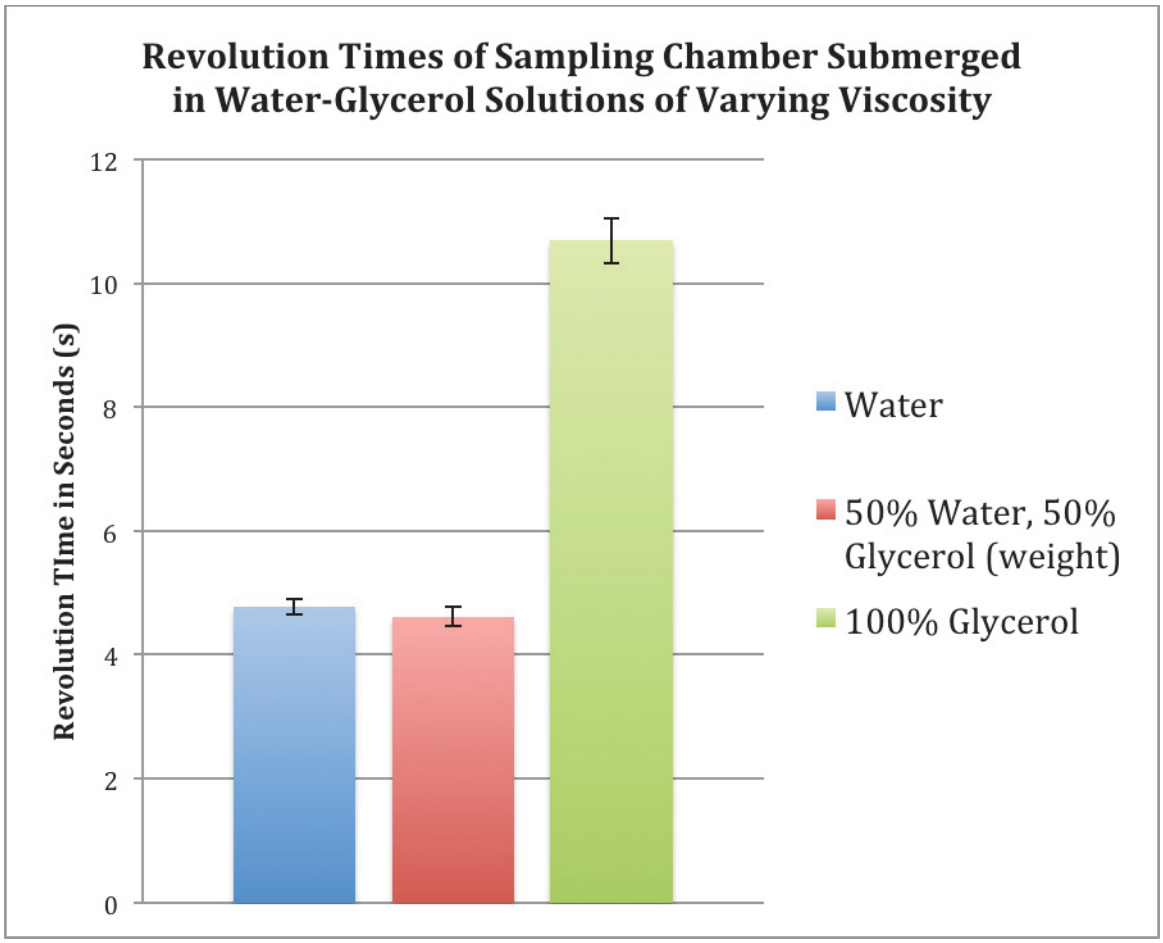

Figure 25: Revolution times of sampling chamber submerged in water-glycerol solutions of varying viscosity

Figure 26: Chamber content composition following sampling and incubation for 1, 2, and 12 hours following HPLC cross-contamination results

5 GENERAL DISCUSSION

The work conducted as part of this research resulted in a candidate device capable of sampling physical samples along the length of the gastrointestinal tract. The latter of two embodiments of the candidate device (i.e. Embodiment B) was selected for continued development due to its simplified construction, robust physical design, and for the extension of its sampling port to the apex of the capsule to better facilitate bulk transfer of material into the chambers. Though the candidate devices developed in this research inherited several aspects from previously developed or proposed ingestible electromechanical capsules, significant departures were made from conventional GI exploration devices in terms of sampling mechanism and sample quantity, form factor, capabilities, and operational workflow. In many of these categories, a clear precedent had not been established and many concepts had not been demonstrated. The unique integration of various, disparate, technologies into a unified device was also in itself a departure. Included in this work was the fabrication of the produced designs and assessment for subsystem integration and operational performance. These assessments yielded promising results and a marked improvement relative to existing/related devices.

Perhaps the most significant design departure was the novel sampling mechanism based on a miniature DC motor positioned along the longitudinal axis of the capsule. Devices proposed in the literature predominantly described the use of vacuous methods such as evacuated chambers or piston/pump mechanisms to draw in luminal content. Microfluidic sampling, to a lesser extent, was also proposed and implemented either in the form of etched microfluidic channels or absorptive fibers and hygroscopic compounds. Both Park and Tang used some form of cyclical motion in their designs for collecting tissue sample from the GI, however Park used rotation to generate linear oscillation that could extend and retract a tissue-grabbing arm into the mucosal wall [94,95]. Tang et al. proposed, but did not demonstrate, counter-rotating blades suited for the biopsy of polyps or other growths protruding into the lumen of the GI [95]. The candidate device produced in this research, however, uses rotary motion to selectively expose sampling chambers. This sampling mechanism demonstrated that reservoirs for samples may be passively filled provided that the openings are sufficiently large. The large port allows for the sampling of a wide

range of fluid viscosities and composition as evidenced in the results of the viscosity test (detailed in Chapter 4) simulating the duodenal contents of the intestinal tract. This is in contrast to the relatively small port sizes of the reviewed devices in the category which were restricted to a narrow range of sample viscosities and were intolerant of particulate matter. The ability to avoid sample bias adds to the quality of data that can be obtained. As there is no phase preference, samples obtained with this device will be more representative of the luminal contents at a given location. To the best of the author's knowledge, this is not something that had previously been reported in this class of device.

Sample volume, quantity of samples, and the quality of the collected samples are differentiating factors of the candidate device developed in this thesis. Each of the three sampling chambers is able to collect 83.8 µL of fluid for a total sample capacity of 251.4 µL. This capacity is comparable to the 262 µL sample (single sample) that was collected by Cui et al. and an order of magnitude greater than the capacity of the microfluidic system proposed by Sprenkels [21,99]. Furthermore, the sampling mechanism of the candidate device is able to fully fill the sampling chambers in a submerged environment whereas the 262 µL sampled by Cui et al. represents only 52% of the designed capacity. The increased sampling efficiency over the previously proposed designs will lead to smaller devices that retain their relatively large sample sizes. Larger sample volumes directly translate to improved laboratory analysis as tests may be performed in replicate and products present in low concentrations will be preserved from downstream dilution/contamination thereby increasing sensitivity. In Chapter 4, the sampling chambers of the candidate device were evaluated for their isolation from one another. The three samples collected in these chambers were shown to be discrete samples with low levels of cross contamination (7.58% over 12-hour time course) that may further be reduced with improved fabrication methods. In the designs reviewed, few have made provisions for sealing the samples from the external environment once they are collected and none have yet quantified the level of cross contamination that occurs. By having quantified the level of cross contamination, and identifying areas for systematically reducing those levels, the candidate GI sampling device is able to provide a level of spatiotemporal resolution previously unattainable.

The control and versatility of the sampling mechanism position the proposed candidate device to become a platform for various forms of gastrointestinal exploration and intervention. Devices described by Howard, Cui, and Sprenkels use enteric plugs as 'triggers' that initiate the sampling, but are unable to control any further aspects of the sampling process [21,98,99]. This uncontrolled sampling is characteristic of the reviewed devices and in practice, would lead to inconsistent results. Test results show that the candidate device developed in this thesis was able to accurately align the sampling port with the sampling chambers in accordance with the times specified in the software. The operator, prior to administration, may explicitly specify the time of sample collection, and the duration of sample chamber exposure. Sampling duration and intestinal motility indicate the length of GI tract represented in a given sample. The operator is able to set run-time parameters prior to administration and download logged data following device retrieval through the UART/USART communication protocol implemented with infrared transceivers. The limitation of an infrared transceiver for communication is that the device requires line-of-sight with the programmer and is unable to transmit data while transiting through the GI tract. This does not have an adverse effect on the operational workflow of the device. Unlike endoscopic capsules that depend on wireless RF communication with an external device to store captured images, the candidate device is retrieved following transit and may thus record transit data internally.

The current embodiment of the candidate device is not designed for histological sampling from the intestinal wall. In fact, it is designed to avoid such interaction with the tissue for safety considerations. It is, however, envisioned that a sampling chamber could be equipped with a brush to better sample the mucosal lining on the GI and further investigate the resident microflora.

6 CONCLUSIONS AND FUTURE DIRECTIONS

This research identified a gap in the existing modalities of gastrointestinal exploration and intervention and demonstrated the need for a new class of device to advance the understanding of the human gastrointestinal tract and for the development of novel therapies for a host of inflammatory, chronic, and metabolic diseases. Existing methods do not fulfill this role as they are either too time consuming and invasive, rendering them ineffective for high throughput testing, fail to preserve the representativeness of the samples, or provide insufficient spatial and temporal information. Next-generation discoveries and treatments require a convenient and low-cost means of exploring bacterial populations, metabolic processes, biochemical markers, and their relationship with diseases. Representative samples must be collected from the lumen of the gastrointestinal tract to give researchers insight into the processes occurring at those sites and to provide feedback on experiments targeting these areas.

Past attempts at solving this problem were investigated by reviewing related devices in the academic literature as well as proposed devices in the patent space. Several designs were attempted and many of the proposed designs were found to be ill suited to the task due to inefficacious sample collection and preservation. Failing to find viable solutions in the literary and patent space, a new class of device was developed. The requirements for this new class of device were established, and a candidate device was developed and tested. The candidate device utilized a novel rotary collection mechanism and the natural musculature of the digestive tract in peristalsis to transfer bulk material of the intestinal lumen into the sampling chambers. Tests were conducted to evaluate the efficacy of the rotary sampling method in collecting and maintaining discrete samples. It was able to collect multiple heterogeneous samples of varying consistencies and maintain a very low level of cross contamination. Tests also showed that it was able to withstand the stresses endured during transit and incidental mechanical shocks.

The modular nature of the resulting design facilitates the continuous enhancement or modification of subcomponents to suit the specified application. Three broad categories for continued development include: the power supply which must be continuously improved for extended battery life and miniaturization, this includes aspects of electrical

and software design; the mechanical strategy to reduce the bulk dimensions of the device and to further optimize the collection mechanism; and finally, the localization strategy to augment capabilities beyond basic transit timing.

Though further work remains to be done, such as the *in-vivo* characterization of the candidate device, the work presented in this thesis: demonstrates the need for such an ingestible and autonomous gastrointestinal sampling device; details the design of its mechanical, electrical, and software components; and demonstrates its feasibility and efficacy in collecting samples *in vitro* and preserving the information within. The applications for this new device class are numerous and its adoption as a platform would have significant impact in this field of research helping to further the study of GI physiology, development in personalized medicine, drug delivery and GI intervention.

APPENDIX

6.1 Bill of Materials (Embodiment A)

Item #	Component	Quantity	Dimensions (mm)	Weight (mg)
1	8-bit Microcontroller	1	3 x 3 x 0.9	7.857
2	High-current analog switch	1	1.25 x 1.00 x 0.60	0.7275
3	NC Magnetic Reed Switch	1	5.5 x 2.2 x 1.8	21.127
4	Blue LED 2.85V	1	1.6 x 0.8 x 0.3	0.3456
5	Hall Effect Switch	1	2 x 2 x 0.5	1.8
6	950nm IR Phototransistor	1	2.5 x 2 x 2.7	2.18
7	2K2 1/5W Resistor	1	1.60 x 0.80 x 0.55	5.13
8	51K 1/10W Resistor	1	1.60 x 0.80 x 0.55	5.13
9	0.1UF 16V Ceramic Capacitor	1	1.60 x 0.80 x 0.55	2.18
10	3.7V 20mAh Lithium polymer cell	1	11 x 17 x 3	800
11	Planetary Geared DC Pager Motor	1	⌀ 6 x 19.2	1200
12	Gold Plated Neodymium Magnet	1	⌀ 1.5 x 0.75	23
13	Plastic Selector Cap	1	⌀ 11 x 16.5	370
14	Plastic End Cap	1	⌀ 11 x 14.5	445
15	Plastic Sampling Chamber	1	⌀ 10 x 14.2	260
16	Rigid PCB	1	9.5 x 12 x 0.79	150

6.2 Bill of Materials (Embodiment B)

Item #	Component	Quantity	Dimensions (mm)	Weight (mg)
1	Microcontroller	1	4x4x0.75	11.64
2	Motor Driver	1	2x2x0.55	2.134
3	IR Emitter/Receiver	2	3.2x1.7x1.1	5.80448
4	Lithium Battery	1	⌀ 10x2.5	700
5	Silver Oxide Battery	1	⌀ 9.5x2.05	610
6	Indicator LED	1	1.6x0.8x0.3	0.3456
7	Magnetic Reed Switch	1	5.5x2.2x1.8	21.127
8	MEMS Magnetic Switch	1	1.8x1.8x0.5	1.5714
9	Secondary High Current Switch	1	1.25x1.00x0.60	0.7275
10	Resistor 100 Kohm	2	1.60x0.80x0.55	2.18
11	Resistor 180 ohm	2	1.60x0.80x0.55	2.18
12	Resistor 1 ohm	1	1.60x0.80x0.55	2.18
13	Resistor 4.7 Kohm	1	1.60x0.80x0.55	2.18
14	Resistor 300 ohm	1	1.60x0.80x0.55	2.18
15	Capacitor 1uF	1	1.60x0.80x0.55	2.18
16	Capacitor 10uF	1	1.60x0.80x0.55	2.18
17	Polycarbonate Exterior Shell	1	⌀ 13.65x29.46	1148
18	Polycarbonate End Cap	1	⌀ 12.5x7.5	322
19	LSR Sampling Chamber	1	⌀ 11.7x15.79	825
20	Motor	1	⌀ 6.0x18.7	1200
21	Flexible PCB	1	10x35x0.1	150

6.3 Firmware Sample

```
/*
 *  avrPill.c
 *
 *  Created: 19/06/2012
 *  Author: Yaw Amoako-Tuffour     [ yaw@micropharma.net ]
 *
 *  Description: Main runtime routine for sampling device
 *
 *  Revisions: Refer to git repository
 *
 */


/*
====================================================================
    SET THESE VALUES !!!!! (Preprocessor Directive Variables)
====================================================================
The following files also require values to be set:

infrared.c  --> THRESHOLD, LIMIT, TIME
motor.c     --> SMPLTIME, SHUNT, MAXCURRENT, MAXTRY, COUNT, BASEPWM

*/

// UNCOMMENT THE VERSION TO RUN

//#define PILLA     // stays open for 4 minutes
//#define PILLB     // stays open for 8 minutes
#define TEST        // each step is 1 minute apart


// Activation Delay
#define activation_delay    10  // delay from removal of magnet, to the beginning
    of the program
                                // a time offset (in minutes) that will be added
                                    to the other values

#ifdef PILLA

    // Sample 1 Collection Time
    #define smpl1_open_hour     (0) // absolute time delays for opening
    #define smpl1_open_min      (15 + activation_delay)
    #define smpl1_close_hour    (0) // absolute time delay for closing
    #define smpl1_close_min     (19 + activation_delay) // Pill A = +4 Pill B= +8


    // Sample 2 Collection Time
    #define smpl2_open_hour     (4) // absolute time delays for opening
    #define smpl2_open_min      (0 + activation_delay)
    #define smpl2_close_hour    (4) // absolute time delay for closing
    #define smpl2_close_min     (4 + activation_delay) // Pill A = +4 Pill B= +8


    // Sample 3 Collection Time
    #define smpl3_open_hour     (8) // absolute time delays for opening
    #define smpl3_open_min      (0 + activation_delay)
    #define smpl3_close_hour    (8) // absolute time delay for closing
    #define smpl3_close_min     (4 + activation_delay) // Pill A = +4 Pill B= +8

#endif

#ifdef PILLB
    // Sample 1 Collection Time
    #define smpl1_open_hour     (0) // absolute time delays for opening
    #define smpl1_open_min      (15 + activation_delay)
    #define smpl1_close_hour    (0) // absolute time delay for closing
    #define smpl1_close_min     (23 + activation_delay) // Pill A = +4 Pill B= +8

    // Sample 2 Collection Time
    #define smpl2_open_hour     (4) // absolute time delays for opening
    #define smpl2_open_min      (0 + activation_delay)
    #define smpl2_close_hour    (4) // absolute time delay for closing
    #define smpl2_close_min     (8 + activation_delay) // Pill A = +4 Pill B= +8

    // Sample 3 Collection Time
    #define smpl3_open_hour     (8) // absolute time delays for opening
    #define smpl3_open_min      (0 + activation_delay)
    #define smpl3_close_hour    (8) // absolute time delay for closing
    #define smpl3_close_min     (8 + activation_delay) // Pill A = +4 Pill B= +8

#endif

#ifdef TEST

    // Sample 1 Collection Time
    #define smpl1_open_hour     (0) // absolute time delays for opening
    #define smpl1_open_min      (1)
    #define smpl1_close_hour    (0) // absolute time delay for closing
    #define smpl1_close_min     (2) // Pill A = +4 Pill B= +8

    // Sample 2 Collection Time
    #define smpl2_open_hour     (0) // absolute time delays for opening
    #define smpl2_open_min      (3)
    #define smpl2_close_hour    (0) // absolute time delay for closing
    #define smpl2_close_min     (4) // Pill A = +4 Pill B= +8

    // Sample 3 Collection Time
    #define smpl3_open_hour     (0) // absolute time delays for opening
    #define smpl3_open_min      (5)
    #define smpl3_close_hour    (0) // absolute time delay for closing
    #define smpl3_close_min     (6) // Pill A = +4 Pill B= +8

#endif


/*
====================================================================
ATTiny24A/44A/84A Pin Configuration
====================================================================
                                          ___________
                                VCC ----|*          |---- GND
    Indicator LED       <-      PB0 ----|           |---- PA0 (ADC0) -> Current
        Sense Hi
    Hall Effect Sensor  <-          PB1 ----|           |---- PA1 (ADC1) -> Current
        Sense Lo
                                    PB3 ----|           |---- PA2 (ADC2) ->
                                      Communications Sense (RX)
    Motor PWM Leg A     <-  (OC0A)  PB2 ----|           |---- PA3        ->
        Communications LED (TX)
    Motor PWM Leg B     <-  (OC0B)  PA7 ----|           |---- PA4 (ADC4) -> Optical
        Encoder Sense
    Optional pH Sense   <-  (ADC6)  PA6 ----|___________|---- PA5        -> Optical
        Encoder LED

    See pins.h for most up-to-date version
*/

/*
====================================================================
    Sampling Routine: Corrected Version, Results in Proper Alignment
====================================================================

    NOTE: FRAME OF REFERENCE ------->
    >> RED Motor Terminal connects to FRONT/TOP
    >> BLUE Motor Terminal connects to BACK/BOTTOM of board
    >>  Forward Direction corresponds with clockwise motion of the MOTOR BODY and
        JUICER
    when looking at the motor from the rear

    0  Initial Position, Closed
    1   0 --> 1 [Open]      [Reverse]   [Sample 1 Open]
    2   1 --> 0 [Closed]    [Forward]   [Sample 2 Closed]
    3   0 --> 4 [Open]      [Forward]   [Sample 2 Open]
    4   4 --> 3 [Closed]    [Forward]   [Sample 2 Closed]
    5   3 --> 2 [Open]      [Forward]   [Sample 3 Open]
    6   2 --> 3 [Closed]    [Reverse]   [Sample 3 Closed]

*/


//====================================
//  HEADER FILES
//====================================

// avr libc header files
#include <avr/io.h>
#include <avr/sleep.h>
#include <avr/eeprom.h>
#include <avr/interrupt.h>

#define F_CPU 1000000UL   //1MHz MICROCONTROLLER OPERATING FREQUENCY
#include <util/delay.h>

// custom header files
#include "modules/time.h"
#include "modules/adc.h"
#include "modules/infrared.h"
#include "modules/motor.h"
#include "modules/power.h"
#include "modules/pins.h"


//====================================
//  NON-VOLATILE TIME MANAGEMENT
//====================================
/*
    - COUNTER increments every 12 seconds, once it reaches 5 counts then
        CLOCK_MIN is incremented
    - CLOCK_MIN increments every minute once it reaches 60 then CLOCK_HOUR is
        incremented
*/

int EEMEM COUNTER;      //increments every 12 seconds, once it reaches 5 it
    increments the minute tab
int EEMEM CLOCK_HOUR;   //main clock hours
int EEMEM CLOCK_MIN;    //main clock minutes

int EEMEM T1_OPEN_HOUR;     //time delay for sample 1 hours
int EEMEM T1_OPEN_MIN;      //time delay for sample 1 minutes
int EEMEM T1_CLOSE_HOUR;    //closing time for sample 1 (hours)
int EEMEM T1_CLOSE_MIN;     //closing time for sample 1 (minutes)

int EEMEM T2_OPEN_HOUR;     //time delay for sample 2 (hours)
int EEMEM T2_OPEN_MIN;      //time delay for sample 2 (minutes)
int EEMEM T2_CLOSE_HOUR;    //closing time for sample 2 (hours)
int EEMEM T2_CLOSE_MIN;     //closing time for sample 2 (minutes)

int EEMEM T3_OPEN_HOUR;     //time delay for sample 3 hours
int EEMEM T3_OPEN_MIN;      //time delay for sample 3 minutes
int EEMEM T3_CLOSE_HOUR;    //closing time for sample 3 (hours)
int EEMEM T3_CLOSE_MIN;     //closing time for sample 3 (minutes)

uint8_t EEMEM STEP;         //helps with timing between motor actuations

//====================================
//  NON-VOLATILE REGISTERS
//====================================
uint8_t EEMEM POSITION          ;   // Keeps track of the position of the
    sampling chamber w.r.t the port
uint8_t EEMEM STATUS[6]         ;   // Status register, non-volatile backup of
    the status register
//uint8_t EEMEM ERRORLOG[6][50] ;   // matrix in which each row contains the
    status register and the error code that caused the state entry

uint8_t EEMEM SAMPLING          ;   // Flag that indicates that device is
    currently opening and/or taking a sample
uint8_t EEMEM CLOSING           ;   // Flag that indicates that device is closing

uint8_t EEMEM COMPLETE          ;   // Flag that indicates that the program is
    complete

//====================================
//  AUTO-TUNING
```

```
//====================================
int EEMEM ADC_MAX               ; // value read when castellation is over the
    sensor
int EEMEM ADC_MIN               ; // value that is read between the castellations

//====================================
//  LOCAL FUNCTION DECLARATIONS
//====================================
void feedback(int num);         // provides visual feedback through LEDs
void initialize_device(void);   // initializes the device
void reset_type(void);          // determines the type of reset that has occurred
void controller(void);          // master switch statement (main control
    structure)
void log_error(void);           // identifies and logs any errors which may arise
uint8_t communication(void);
void autotune(void);


//=========================================================================
//  MAIN PROGRAM ENTRY POINT
//=========================================================================
int main(void)
{

    adc_on();               // turn on ADC, essential for reset type
        determination

    reset_type();           // determine between an intentional reset and a soft
        reset

    start_chrono();         // start the 16-bit timer (12-second interrupt)

    while(1){
        controller();       // determines the next action of micro-controller
            based on EEPROM
    }


} //end of main loop


//=========================================================================
//  INTERRUPT SERVICE ROUTINE
//=========================================================================

ISR(TIM1_COMPA_vect)
{
    //indicator LED blink every 12 seconds to show that power is applied
    PORTB |=(1<<led_aux);
    _delay_ms(50);
    PORTB &= ~(1<<led_aux);

    //variable declaration
    int counter = 0;
    int clock_hour = 0;
    int clock_min = 0;
```

```
    int t1_open_hour=0;
    int t1_open_min=0;
    int t2_open_hour=0;
    int t2_open_min=0;
    int t3_open_hour=0;
    int t3_open_min=0;

    int t1_close_hour = 0;
    int t1_close_min = 0;
    int t2_close_hour = 0;
    int t2_close_min = 0;
    int t3_close_hour = 0;
    int t3_close_min = 0;

    int state = 0;  //checks the state, makes necessary adjustments if necessary
    int status = 0;

    int sampling = 0;   // flag to indicate currently opening/sampling
    int closing = 0;    // flag to indicate currently closing

    int step = 0;

    //assignment - load values from non-volatile memory
    counter = eeprom_read_byte(&COUNTER);
    clock_hour = eeprom_read_byte(&CLOCK_HOUR);
    clock_min = eeprom_read_byte(&CLOCK_MIN);

    t1_open_hour = eeprom_read_byte(&T1_OPEN_HOUR);
    t1_open_min = eeprom_read_byte(&T1_OPEN_MIN);
    t2_open_hour = eeprom_read_byte(&T2_OPEN_HOUR);
    t2_open_min = eeprom_read_byte(&T2_OPEN_MIN);
    t3_open_hour = eeprom_read_byte(&T3_OPEN_HOUR);
    t3_open_min = eeprom_read_byte(&T3_OPEN_MIN);

    t1_close_hour = eeprom_read_byte(&T1_CLOSE_HOUR);
    t1_close_min = eeprom_read_byte(&T1_CLOSE_MIN);
    t2_close_hour = eeprom_read_byte(&T2_CLOSE_HOUR);
    t2_close_min = eeprom_read_byte(&T2_CLOSE_MIN);
    t3_close_hour = eeprom_read_byte(&T3_CLOSE_HOUR);
    t3_close_min = eeprom_read_byte(&T3_CLOSE_MIN);

    status = eeprom_read_byte(&STATUS);

    step = eeprom_read_byte(&STEP);

    //update times - make the necessary increments
    counter++;

    if (counter==5)
    {
        counter = 0;        //reset the counter
        clock_min++;        //increment the minutes if the counter has reached 5

        if (clock_min==60)
        {
```

```
            clock_min = 0;  //reset the minutes
            clock_hour++;   //increment the hour if the minutes have reached 60
        }
    }

    eeprom_update_byte(&COUNTER,counter);       //commit to eeprom if there are
        changes
    eeprom_update_byte(&CLOCK_MIN, clock_min);
    eeprom_update_byte(&CLOCK_HOUR, clock_hour);

    //comparison - if operation is normal, then compare clock to sampling times

    if ((clock_hour==t1_open_hour)&&(clock_min==t1_open_min))                //
        SMPL #1 Opening
    {
        sampling = eeprom_read_byte(&SAMPLING);
        if(!(sampling==1))
        {
            eeprom_update_byte(&SAMPLING,1);
            eeprom_update_byte(&CLOSING,0);
            eeprom_update_byte(&STEP,1);
        }
    }
    else if((clock_hour==t1_close_hour)&&(clock_min==t1_close_min))         //
        SMPL #1 Closing
    {
        closing = eeprom_read_byte(&CLOSING);
        if(!(closing==1))
        {
            eeprom_update_byte(&SAMPLING,0);    //clear the sampling flag
            eeprom_update_byte(&CLOSING,1);     //set the closing flag
            eeprom_update_byte(&STEP,2);
        }
    }
    else if ((clock_hour==t2_open_hour)&&(clock_min==t2_open_min))          //
        SMPL #2 Opening
    {
        sampling = eeprom_read_byte(&SAMPLING);
        if(!(sampling==1))
        {
            eeprom_update_byte(&SAMPLING,1);    //set the sampling flag
            eeprom_update_byte(&CLOSING,0);     //clear the closing flag
            eeprom_update_byte(&STEP,3);
        }
    }
    else if((clock_hour==t2_close_hour)&&(clock_min==t2_close_min))         //
        SMPL #2 Closing
    {
        closing = eeprom_read_byte(&CLOSING);
        if(!(closing==1))
        {
            eeprom_update_byte(&SAMPLING,0);    //clear the sampling flag
            eeprom_update_byte(&CLOSING,1);     //set the closing flag
            eeprom_update_byte(&STEP,4);
        }
    }
```

```
    else if ((clock_hour==t3_open_hour)&&(clock_min==t3_open_min))          //
        SMPL #3 Opening
    {
        sampling = eeprom_read_byte(&SAMPLING);
        if(!(sampling==1))
        {
            eeprom_update_byte(&SAMPLING,1);    //set the sampling flag
            eeprom_update_byte(&CLOSING,0);     //clear the closing flag
            eeprom_update_byte(&STEP,5);
        }
    }
    else if((clock_hour==t3_close_hour)&&(clock_min==t3_close_min))         //
        SMPL #3 Closing
    {
        closing = eeprom_read_byte(&CLOSING);
        if(!(closing==1))
        {
            eeprom_update_byte(&SAMPLING,0);    //clear the sampling flag
            eeprom_update_byte(&CLOSING,1);     //set the closing flag
            eeprom_update_byte(&STEP,6);
        }
    }
    else if(step==0)
    {
        eeprom_update_byte(&SAMPLING,0);
        eeprom_update_byte(&CLOSING,0);
        eeprom_update_byte(&STEP,0);
    }

}


//=========================================================================
//  LOCAL FUNCTION DEFINITIONS
//=========================================================================

void feedback(int num){
    while (num>0)
    {
        PORTB |= (1<<led_aux);
        _delay_ms(300);
        PORTB &= ~(1<<led_aux);
        _delay_ms(200);
        num--;
    }

    _delay_ms(500);
}

//  1st function called in firmware: determines the type of reset applied
    (intentional or brief disconnect)
void reset_type(void){
    int temp=0;
    int value=0;
    int flag =0;
```

REFERENCES

1. Everhart JE, Ruhl CE. Burden of digestive diseases in the United States part I: overall and upper gastrointestinal diseases. *Gastroenterology*. 2009;136(2):376–386.

2. Peery AF, Dellon ES, Lund J, Crockett SD, McGowan CE, Bulsiewicz WJ, Gangarosa LM, Thiny MT, Stizenberg K, Morgan DR. Burden of gastrointestinal disease in the United States: 2012 update. *Gastroenterology*. 2012.

3. Tang WHW, Wang Z, Levison BS, Koeth RA, Britt EB, Fu X, Wu Y, Hazen SL. Intestinal Microbial Metabolism of Phosphatidylcholine and Cardiovascular Risk. *The New England journal of medicine*. 2013;368(17):1575–1584.

4. Ouwehand A, Isolauri E, Salminen S. The role of the intestinal microflora for the development of the immune system in early childhood. *European journal of nutrition*. 2002;41(1):i32–i37.

5. Neish AS. Microbes in gastrointestinal health and disease. *Gastroenterology*. 2009;136(1):65–80.

6. Painter J, Saunders D, Bell GD, Williams C, Pitt R, Bladen J. Depth of insertion at flexible sigmoidoscopy: implications for colorectal cancer screening and instrument design. *Endoscopy*. 1999;31(03):227–231.

7. May A, Nachbar L, Schneider M, Neumann M, Ell C. Push-and-pull enteroscopy using the double-balloon technique: method of assessing depth of insertion and training of the enteroscopy technique using the Erlangen Endo-Trainer. *Endoscopy*. 2005;37(01):66–70.

8. Yamamoto H, Sekine Y, Sato Y, Higashizawa T, Miyata T, Iino S, Ido K, Sugano K. Total enteroscopy with a nonsurgical steerable double-balloon method. *Gastrointestinal endoscopy*. 2001;53(2):216–220.

9. Yamamoto H KH. Double-balloon endoscopy. *Current opinion in gastroenterology*. 2005;21(5):573–7.

10. Mehdizadeh S, Ross A, Gerson L, Leighton J, Chen A, Schembre D, Chen G, Semrad C, Kamal A, Harrison EM. What is the learning curve associated with double-balloon enteroscopy? Technical details and early experience in 6 US tertiary care centers. *Gastrointestinal endoscopy*. 2006;64(5):740–750.

11. Morikawa T, Kato J, Yamaji Y, Wada R, Mitsushima T, Shiratori Y. A Comparison of the Immunochemical Fecal Occult Blood Test and Total Colonoscopy in the Asymptomatic Population. *Gastroenterology*. 129(2):422–428.

12. Zhi J, Melia A, Guerciolini R, Chung J, Kinberg J, Hauptman J, Patel I. Retrospective population-based analysis of the dose-response (fecal fat excretion) relationship of orlistat in normal and obese volunteers. *Clinical Pharmacology & Therapeutics*. 1994;56(1):82–85.

13. Jankowski JA, Odze RD. Biomarkers in gastroenterology: between hope and hype comes histopathology. *The American journal of gastroenterology*. 2009;104(5):1093–1096.

14. Jesudoss P, Mathewson A, Twomey K, Stam F, Wright WM. A swallowable diagnostic capsule with a direct access sensor using Anisotropic Conductive Adhesive. *IEEE Int. Reliab. Phys. Symp. Proc. IEEE International Reliability Physics Symposium Proceedings*. 2011:3B.3.1–3B.3.7.

15. Moglia A, Menciassi A, Dario P. Capsule endoscopy: progress update and challenges ahead. *Nature reviews. Gastroenterology & hepatology*. 2009;6(6):353–62.

16. Lin L, Rasouli M, Kencana AP, Tan SL, Wong KJ, Ho KY, Phee SJ. Capsule endoscopy-A mechatronics perspective. *Front. Mech. Eng. China Frontiers of Mechanical Engineering in China*.

2011;6(1):33–39.

17. McCaffrey C, Chevalerias O, O'Mathuna C, Twomey K. Swallowable-Capsule Technology. *IEEE pervasive computing /*. 2008;7(1):29.

18. Menciassi A, Quirini M, Dario P. Microrobotics for future gastrointestinal endoscopy. *Minimally invasive therapy & allied technologies : MITAT : official journal of the Society for Minimally Invasive Therapy*. 2007;16(2):91–100.

19. Sharma VK. The future is wireless: advances in wireless diagnostic and therapeutic technologies in gastroenterology. *Gastroenterology*. 2009;137(2):434–9.

20. Toennies JL, Tortora G, Simi M, Valdastri P, Webster R. Swallowable medical devices for diagnosis and surgery: the state of the art. *Proceedings of the Institution of Mechanical Engineers, Part C: Journal of Mechanical Engineering Science*. 2010;224(7):1397–1414.

21. Cui J, Zheng X, Hou W, Zhuang Y, Pi X, Yang J. The study of a remote-controlled gastrointestinal drug delivery and sampling system. *Telemedicine journal and e-health : the official journal of the American Telemedicine Association*. 2008;14(7):715–9.

22. Chandrappan J, Ruiqi L, Su N, Yi GHY, Vaidyanathan K. Thermo-mechanical actuator-based miniature tagging module for localization in capsule endoscopy. *J Micromech Microengineering Journal of Micromechanics and Microengineering*. 2011;21(4).

23. Maton A. *Human biology and health*. Englewood Cliffs, N.J.: Prentice Hall; 1993.

24. Ho KK, Joyce AM. Complications of capsule endoscopy. *Gastrointestinal endoscopy clinics of North America*. 2007;17(1):169–178.

25. Cheifetz AS, Kornbluth AA, Legnani P, Schmelkin I, Brown A, Lichtiger S, Lewis BS. The risk of retention of the capsule endoscope in patients with known or suspected Crohn's disease. *The American journal of gastroenterology*. 2006;101(10):2218–2222.

26. Egorov VI, Schastlivtsev IV, Prut EV, Baranov AO, Turusov RA. Mechanical properties of the human gastrointestinal tract. *Journal of biomechanics*. 2002;35(10):1417–1425.

27. Liu H-Y, Wang G, Wei K, Pi X-T, Zhu L, Zheng X-L, Wen Z-Y. An intelligent electronic capsule system for automated detection of gastrointestinal bleeding. *Journal of Zhejiang University. Science. B*. 2010;11(12):937–43.

28. Uehara A, Hoshina K. Capsule endoscope NORIKA system. *Minimally invasive therapy & allied technologies : MITAT : official journal of the Society for Minimally Invasive Therapy*. 2003;12(5):227–234.

29. Gheorghe C, Iacob R, Bancila I. Olympus capsule endoscopy for small bowel examination. *JOURNAL OF GASTROINTESTINAL AND LIVER DISEASES*. 2007;16(3):309–314.

30. Cave D, Legnani P, De Franchis R, Lewis B. ICCE consensus for capsule retention. *Endoscopy*. 2005;37(10):1065–1067.

31. Rondonotti E, Herrerias JM, Pennazio M, Caunedo A, Mascarenhas-Saraiva M, de Franchis R. Complications, limitations, and failures of capsule endoscopy: a review of 733 cases. *Gastrointestinal endoscopy*. 2005;62(5):712–716.

32. Taylor S, Wakem M, Dijkman G, Alsarraj M, Nguyen M. A practical approach to RT-qPCR—publishing data that conform to the MIQE guidelines. *Methods*. 2010;50(4):S1–S5.

33. Williams DF. On the mechanisms of biocompatibility. *Biomaterials*. 2008;29(20):2941–2953.

34. Ratner BD, Bryant SJ. Biomaterials: where we have been and where we are going. *Annu. Rev. Biomed. Eng.* 2004;6:41–75.

35. Scott G. *Why Degradable Polymers?* Springer; 2002.

36. Saad B, Neuenschwander P, Uhlschmid G, Suter U. New versatile, elastomeric, degradable polymeric materials for medicine. *International journal of biological macromolecules*. 1999;25(1):293–301.

37. Han A, Oh KW, Bhansali S, Thurman Henderson H, Ahn CH. A low temperature biochemically compatible bonding technique using fluoropolymers for biochemical microfluidic systems. In: *Micro Electro Mechanical Systems, 2000. MEMS 2000. The Thirteenth Annual International Conference on*. IEEE; 2000:414–418.

38. Valle Della F, Calderini G, Rastrelli A, Romeo A. Biocompatible perforated membranes, processes for their preparation, their use as a support in the in vitro growth of epithelial cells, the artificial skin obtained in this manner, and its use in skin grafts. 1997.

39. Casaletto M, Ingo G, Kaciulis S, Mattogno G, Pandolfi L, Scavia G. Surface studies of in vitro biocompatibility of titanium oxide coatings. *Applied surface science*. 2001;172(1):167–177.

40. Rohr T, Ogletree DF, Svec F, Fréchet JM. Surface functionalization of thermoplastic polymers for the fabrication of microfluidic devices by photoinitiated grafting. *Advanced functional materials*. 2003;13(4):264–270.

41. Heller J. Controlled release of biologically active compounds from bioerodible polymers. *Biomaterials*. 1980;1(1):51–57.

42. Porter S, Ridgway K. The permeability of enteric coatings and the dissolution rates of coated tablets. *Journal of Pharmacy and Pharmacology*. 1982;34(1):5–8.

43. Wang L, Tang TB, Johannessen E, Astaras A, Ahmadian M, Murrary A, Cooper J, Beaumont S, Flynn B, Cumming D. Integrated micro-instrumentation for dynamic monitoring of the gastro-intestinal tract. In: *Microtechnologies in Medicine & Biology 2nd Annual International IEEE-EMB Special Topic Conference on*. IEEE; 2002:219–222.

44. Quirini M, Webster R, Menciassi A, Dario P. Design of a pill-sized 12-legged endoscopic capsule robot. In: *Robotics and Automation, 2007 IEEE International Conference on*. IEEE; 2007:1856–1862.

45. Tortora G, Valdastri P, Susilo E, Menciassi A, Dario P, Rieber F, Schurr MO. Propeller-based wireless device for active capsular endoscopy in the gastric district. *Minimally invasive therapy & allied technologies : MITAT : official journal of the Society for Minimally Invasive Therapy*. 2009;18(5):280–290.

46. Park H, Park S, Yoon E, Kim B, Park J, Park S. Paddling based microrobot for capsule endoscopes. In: *Robotics and Automation, 2007 IEEE International Conference on*. IEEE; 2007:3377–3382.

47. Simi M, Valdastri P, Quaglia C, Menciassi A, Dario P. Design, fabrication, and testing of a capsule with hybrid locomotion for gastrointestinal tract exploration. *Mechatronics, IEEE/ASME Transactions on*. 2010;15(2):170–180.

48. Kim B, Lee S, Park JH, Park J-O. Design and fabrication of a locomotive mechanism for capsule-type endoscopes using shape memory alloys (SMAs). *Mechatronics, IEEE/ASME Transactions on*. 2005;10(1):77–86.

49. Carpi F, Kastelein N, Talcott M, Pappone C. Magnetically controllable gastrointestinal steering of video capsules. *IEEE transactions on bio-medical engineering*. 2011;58(2):231–234.

50. Ciuti G, Valdastri P, Menciassi A, Dario P. Robotic magnetic steering and locomotion of capsule endoscope for diagnostic and surgical endoluminal procedures. *Robotica Robotica*. 2010;28(2):199–207.

51. Sendoh M, Ishiyama K, Arai K-I. Fabrication of magnetic actuator for use in a capsule endoscope. *Magnetics, IEEE Transactions on*. 2003;39(5):3232–3234.

52. Reddy S, Arzt E, del Campo A. Bioinspired surfaces with switchable adhesion. *Advanced Materials*. 2007;19(22):3833–3837.

53. Jeong HE, Kwak MK, Suh KY. Stretchable, adhesion-tunable dry adhesive by surface wrinkling. *Langmuir*. 2010;26(4):2223–2226.

54. Murphy MP, Kim S, Sitti M. Enhanced adhesion by gecko-inspired hierarchical fibrillar adhesives. *ACS applied materials & interfaces*. 2009;1(4):849–855.

55. Standring S. Gray's anatomy. 2008:1111–1137.

56. Bulat J, Duda K, Duplaga M, Fraczek R, Skalski A, Socha M, Turcza P, Zielinski T. Data processing tasks in wireless GI endoscopy: image-based capsule localization & navigation and video compression. In: *Engineering in Medicine and Biology Society, 2007. EMBS 2007. 29th Annual International Conference of the IEEE*. IEEE; 2007:2815–2818.

57. Wang X, Meng M-H, Hu C. A localization method using 3-axis magnetoresistive sensors for tracking of capsule endoscope. In: *Engineering in Medicine and Biology Society, 2006. EMBS'06. 28th Annual International Conference of the IEEE*. IEEE; 2006:2522–2525.

58. Hou J, Zhu Y, Zhang L, Fu Y, Zhao F, Yang L, Rong G. Design and implementation of a high resolution localization system for in-vivo capsule endoscopy. In: *Dependable, Autonomic and Secure Computing, 2009. DASC'09. Eighth IEEE International Conference on*. IEEE; 2009:209–214.

59. Davis S, Hardy J, Fara J. Transit of pharmaceutical dosage forms through the small intestine. *Gut*. 1986;27(8):886–892.

60. Kaler KV, Mintchev MP. Inertial navigation method and apparatus for wireless bolus transit monitoring in gastrointestinal tract. 2005.

61. Tan C-W, Park S. Design of Accelerometer-Based Inertial Navigation Systems. *IEEE TRANSACTIONS ON INSTRUMENTATION AND MEASUREMENT*. 2005;54(6):2520–2530.

62. Barshan B, Durrant-Whyte HF. Inertial navigation systems for mobile robots. *Robotics and Automation, IEEE Transactions on*. 1995;11(3):328–342.

63. Cunha JS, Coimbra M, Campos P, Soares JM. Automated topographic segmentation and transit time estimation in endoscopic capsule exams. *Medical Imaging, IEEE Transactions on*. 2008;27(1):19–27.

64. Li B, Meng MQ-H. Texture analysis for ulcer detection in capsule endoscopy images. *Image and Vision computing*. 2009;27(9):1336–1342.

65. Liu L, Hu C, Cai W, Meng M-H. Capsule endoscope localization based on computer vision technique. In: *Engineering in Medicine and Biology Society, 2009. EMBC 2009. Annual International Conference of the IEEE*. IEEE; 2009:3711–3714.

66. Arshak K, Adepoju F. Adaptive linearized methods for tracking a moving telemetry capsule. In: *Industrial Electronics, 2007. ISIE 2007. IEEE International Symposium on*. IEEE; 2007:2703–2708.

67. Than TD, Alici G, Zhou H, Li W. A review of localization systems for robotic endoscopic capsules. *IEEE transactions on bio-medical engineering*. 2012;59(9):2387–2399.

68. Khan UI, Pahlavan K, Makarov S. Comparison of TOA and RSS based techniques for RF localization inside human tissue. In: *Engineering in Medicine and Biology Society, EMBC, 2011 Annual International Conference of the IEEE*. IEEE; 2011:5602–5607.

69. Nagy Z, Fluckiger M, Ergeneman O, Pané S, Probst M, Nelson BJ. A wireless acoustic emitter for passive localization in liquids. In: *Robotics and Automation, 2009. ICRA'09. IEEE International Conference on*. IEEE; 2009:2593–2598.

70. Prior DV, Connor AL, Wilding IR. The enterion capsule. *DRUGS AND THE PHARMACEUTICAL SCIENCES*. 2003;126:273–288.

71. Mojaverian P. Evaluation of gastrointestinal pH and gastric residence time via the Heidelberg Radiotelemetry Capsule: Pharmaceutical application. *Drug development research*. 1996;38(2):73–85.

72. Sang-Hyo W, Jyung-Hyun L, Min-Kyu K, Chul-Ho W, Jin-Ho C. Telemetry capsule for pressure monitoring in the gastrointestinal tract. *IEICE Transactions on Fundamentals of Electronics, Communications and Computer Sciences*. 2006;89(6):1699–1700.

73. Zhou G-X. Swallowable or implantable body temperature telemeter-body temperature radio pill. In: *Bioengineering Conference, 1989., Proceedings of the 1989 Fifteenth Annual Northeast*. IEEE; 1989:165–166.

74. Cutchis PN, Hogrefe AF, Lesho JC. The ingestible thermal monitoring system. *Johns Hopkins APL Technical Digest*. 1988;9:16–21.

75. Wang L, Johannessen EA, Hammond PA, Cui L, Reid SW, Cooper JM, Cumming DR. A programmable microsystem using system-on-chip for real-time biotelemetry. *IEEE transactions on bio-medical engineering*. 2005;52(7):1251–60.

76. Ask P, Edwall G, Johansson K, Tibbling L. On the use of monocrystalline antimony pH electrodes in gastro-oesophageal functional disorders. *Medical and Biological Engineering and Computing*. 1982;20(3):383–389.

77. Savarino V, Mela G, Zentilin P, Magnolia M, Scalabrint P, Valle F, More'iti M, Bonifacino G, Celle G. Gastric aspiration versus antimony and glass pH electrodes: A simultaneous comparative in vivo study. *Scandinavian journal of gastroenterology*. 1989;24(4):434–439.

78. Wang L, Yang G-Z, Huang J, Zhang J, Yu L, Nie Z, Cumming DRS. A Wireless Biomedical Signal Interface System-on-Chip for Body Sensor Networks. *IEEE transactions on biomedical circuits and systems*. 2010;4(2):112–7.

79. Evans D, Pye G, Bramley R, Clark A, Dyson T, Hardcastle J. Measurement of gastrointestinal pH profiles in normal ambulant human subjects. *Gut*. 1988;29(8):1035–1041.

80. Chiang J-L, Jan S-S, Chou J-C, Chen Y-C. Study on the temperature effect, hysteresis and drift of pH-ISFET devices based on amorphous tungsten oxide. *Sensors and Actuators B: Chemical*. 2001;76(1):624–628.

81. McKenzie J, Osgood D. Validation of a new telemetric core temperature monitor. *Journal of Thermal*

Biology. 2004;29(7):605–611.

82. Tearney G, Brezinski M, Southern J, Bouma B, Boppart S, Fujimoto J. Optical biopsy in human gastrointestinal tissue using optical coherence tomography. *The American journal of gastroenterology*. 1997;92(10):1800–1804.

83. Shim MG, Wong Kee Song L-M, Marcon NE, Wilson BC. In vivo Near-infrared Raman Spectroscopy: Demonstration of Feasibility During Clinical Gastrointestinal Endoscopy¶. *Photochemistry and photobiology*. 2000;72(1):146–150.

84. Gong F, Swain P, Mills T. Wireless endoscopy. *Gastrointestinal endoscopy*. 2000;51(6):725–729.

85. Iddan G, Meron G, Glukhovsky A, Swain P. Wireless capsule endoscopy. *Nature*. 2000;405:417.

86. Savci HS, Sula A, Wang Z, Dogan NS, Arvas E. MICS transceivers: regulatory standards and applications [medical implant communications service]. In: *SoutheastCon, 2005. Proceedings. IEEE*. IEEE; 2005:179–182.

87. Zhen B, Li H-B, Kohno R. IEEE body area networks and medical implant communications. In: *Proceedings of the ICST 3rd international conference on Body area networks*. ICST (Institute for Computer Sciences, Social-Informatics and Telecommunications Engineering); 2008:26.

88. Schmidt CL, Skarstad PM. The future of lithium and lithium-ion batteries in implantable medical devices. *Journal of power sources*. 2001;97:742–746.

89. Takeuchi KJ, Leising RA, Palazzo MJ, Marschilok AC, Takeuchi ES. Advanced lithium batteries for implantable medical devices: mechanistic study of SVO cathode synthesis. *Journal of power sources*. 2003;119:973–978.

90. Lenaerts B, Puers R. An inductive power link for a wireless endoscope. *Biosensors and Bioelectronics*. 2007;22(7):1390–1395.

91. Carta R, Thoné J, Puers R. A wireless power supply system for robotic capsular endoscopes. *Sensors and Actuators A: Physical Sensors and Actuators A: Physical*. 2010;162(2):177–183.

92. Crosby WH, Army U, Kugler HW. Intraluminal biopsy of the small intestine. *Digestive diseases and sciences*. 1957;2(5):236–241.

93. Prout B. A rapid method of obtaining a jejunal biopsy using a Crosby capsule and a gastrointestinal fiberscope. *Gut*. 1974;15(7):571–572.

94. Park S, Koo K-I, Bang SM, Park JY, Song SY. A novel microactuator for microbiopsy in capsular endoscopes. *J Micromech Microengineering Journal of Micromechanics and Microengineering*. 2008;18(2).

95. Tang J, Wang L, Ying J, Lee W, Ho P. Apparatus and methods of using built-in micro-spectroscopy micro-biosensors and specimen collection system for a wireless capsule in a biological body in vivo. 2003.

96. Tsai N-C, Sue C-Y. Review of MEMS-based drug delivery and dosing systems. *Sensors and Actuators A: Physical Sensors and Actuators A: Physical*. 2007;134(2):555–564.

97. Zengerle R, Ulrich J, Kluge S, Richter M, Richter A. A bidirectional silicon micropump. *Sensors and Actuators A: Physical Sensors and Actuators A: Physical*. 1995;50(1):81–86.

98. Gu HH, Gu HL. Intestinal fluid sampler. 1999.

99. SPRENKELS A, JENNEBOER A, Johannes S, VENEMA K, van den BERG A, DE VOS W. SAMPLING DEVICE FOR IN VIVO SAMPLING OF LIQUIDS FROM THE GASTROINTESTINAL TRACT, PROCESS FOR THE PRODUCTION THEREOF AND MOULD OR MASK FOR USE IN THE PRODUCTION PROCESS. 2007.

100. Borgström B, Dahlqvist A, Lundh G, Sjövall J. Studies of intestinal digestion and absorption in the human. *Journal of Clinical Investigation*. 1957;36(10):1521.

101. Savage DC. Microbial ecology of the gastrointestinal tract. *Annual Reviews in Microbiology*. 1977;31(1):107–133.

102. Kararli TT. Comparison of the gastrointestinal anatomy, physiology, and biochemistry of humans and commonly used laboratory animals. *Biopharmaceutics & drug disposition*. 1995;16(5):351–80.

103. Corfield A, Myerscough N, Longman R, Sylvester P, Arul S, Pignatelli M. Mucins and mucosal protection in the gastrointestinal tract: new prospects for mucins in the pathology of gastrointestinal disease. *Gut*. 2000;47(4):589–594.

104. Hillemeier C. An overview of the effects of dietary fiber on gastrointestinal transit. *Pediatrics*. 1995;96(5):997–9.

105. Hao W-L, Lee Y-K. Microflora of the gastrointestinal tract: a review. *Methods in molecular biology (Clifton, N.J.)*. 2004;268:491–502.

106. Rakoff-Nahoum S, Paglino J, Eslami-Varzaneh F, Edberg S, Medzhitov R. Recognition of commensal microflora by toll-like receptors is required for intestinal homeostasis. *Cell*. 2004;118(2):229–241.

107. Macfarlane G, Allison C, Gibson S, Cummings J. Contribution of the microflora to proteolysis in the human large intestine. *Journal of Applied Microbiology*. 1988;64(1):37–46.

108. Albert M, Mathan V, Baker S. Vitamin B12 synthesis by human small intestinal bacteria. 1980.

109. Hill M. Intestinal flora and endogenous vitamin synthesis. *European Journal of Cancer Prevention*. 1997;6(2):S43–S45.

110. Burkholder PR, McVeigh I. Synthesis of vitamins by intestinal bacteria. *Proceedings of the National Academy of Sciences of the United States of America*. 1942;28(7):285.

111. Berg RD. The indigenous gastrointestinal microflora. *Trends in microbiology*. 1996;4(11):430–5.

112. Ciancio SG, Mather ML, Zambon JJ, Reynolds HS. Effect of a chemotherapeutic agent delivered by an oral irrigation device on plaque, gingivitis, and subgingival microflora. *Journal of periodontology*. 1989;60(6):310–315.

113. Edlund C, Nord CE. Effect on the human normal microflora of oral antibiotics for treatment of urinary tract infections. *Journal of Antimicrobial Chemotherapy*. 2000;46(suppl 1):41–48.

114. Turnbaugh PJ, Ridaura VK, Faith JJ, Rey FE, Knight R, Gordon JI. The effect of diet on the human gut microbiome: a metagenomic analysis in humanized gnotobiotic mice. *Science translational medicine*. 2009;1(6):6ra14.

115. Gazzaniga A, Iamartino P, Maffione G, Sangalli M. Oral delayed-release system for colonic specific delivery. *International Journal of Pharmaceutics*. 1994;108(1):77–83.

116. Kim K, Won K, Shin J, Choi H-J. A comparison of communication techniques for capsule

endoscopes. In: *Communications (APCC), 2011 17th Asia-Pacific Conference on*. IEEE; 2011:761–764.

117. Layton A, McKay L, Williams D, Garrett V, Gentry R, Sayler G. Development of Bacteroides 16S rRNA gene TaqMan-based real-time PCR assays for estimation of total, human, and bovine fecal pollution in water. *Applied and Environmental Microbiology*. 2006;72(6):4214–4224.

118. Dodds W, Stef J, Hogan W, Hoke S, Stewart E, Arndorfer R. Radial distribution of esophageal peristaltic pressure in normal subjects and patients with esophageal diverticulum. *Gastroenterology*. 1975;69(3):584.

119. Clouse R, Staiano A. Topography of the esophageal peristaltic pressure wave. *American Journal of Physiology-Gastrointestinal and Liver Physiology*. 1991;261(4):G677–G684.

120. Humphries TJ, Castell DO. Pressure profile of esophageal peristalsis in normal humans as measured by direct intraesophageal transducers. *The American journal of digestive diseases*. 1977;22(7):641–645.

121. Tay ET, Weinberg G, Levin TL. Ingested magnets: the force within. *Pediatric emergency care*. 2004;20(7):466–467.

122. Nui A, Hirama T, Katsuramaki T, Maeda T, Meguro M, Nagayama M, Matsuno T, Mizumoto T, Hirata K. An intestinal volvulus caused by multiple magnet ingestion: an unexpected risk in children. *Journal of pediatric surgery*. 2005;40(9):e9–e11.

123. Olson J, Whitney DH, Durkee K, Shuber AP. DNA stabilization is critical for maximizing performance of fecal DNA-based colorectal cancer tests. *Diagnostic Molecular Pathology*. 2005;14(3):183–191.

124. Jones ML, Chen H, Ouyang W, Metz T, Prakash S. Method for bile acid determination by high performance liquid chromatography. *JOURNAL OF MEDICAL SCIENCES-TAIPEI*. 2003;23(5):277–280.

125. Kong F, Singh R. Disintegration of solid foods in human stomach. *Journal of food science*. 2008;73(5):R67–R80.

126. Kwon K, Pallerla S. Viscosity of glycerol and its aqueous solutions measured by a tank-tube viscometer. *Chemical Engineering Communications*. 2000;183(1):71–97.

127. Kamba M, Seta Y, Kusai A, Ikeda M, Nishimura K. A unique dosage form to evaluate the mechanical destructive force in the gastrointestinal tract. *International Journal of Pharmaceutics*. 2000;208(1):61–70.